New Preparation Technique for Titanium Dioxide Photocatalyst and its Application to Surface Treatment

YOSHIE ISHIKAWA

Graduate School of Science and Technology
Kumamoto University

2003

PREFACE

TiO_2 photocatalytic technology is very attractive for both academic and industrial fields, because TiO_2 photocatalytic processes under UV illumination show potentially advantages in several active areas, such as antibacterial action, environmental clean-up and solar energy conversion. Various commercial products where photocatalytic function is added have been developed. Therefore, the study of the preparation and fixation method of TiO_2 is very important.

In this thesis, the electrochemical preparation of TiO_2 photocatalyst film on alumite substrate ($Al/Al_2O_3/TiO_2$) are demonstrated, and then the photocatalytic activity and characterization of the prepared $Al/Al_2O_3/TiO_2$ are discussed.

Moreover, the surface treatment of inorganic materials such as silicon carbide and diamond using TiO_2 photocatalyst as a new utility of TiO_2 photocatalyst is also discussed.

Chapter 1 Introduction

In this chapter, the general background of present thesis and aims of the present studies are described.

Part I: Preparation of TiO_2 photocatalyst on alumite substrate.

Chapter 2 A New Electrochemical Method to Prepare Mesoporous Titanium(IV) Oxide Photocatalyst Fixed on Alumite Substrate

The electrochemical method consisting of a two-step electrolysis to prepare the TiO_2 film fixed on alumite is described. The characterization and photoatcalytic activity of the prepared TiO_2 film are demonstrated. Moreover, the deposition mechanism is

discussed. The contents of this chapter are based on the following published papers:

Y. Matsumoto, C. Nakanishi, Y. Ishikawa, M. Koinuma and N. Yatsushiro
"Photocatalytic Activity of Alumite Fixed with TiO_2"
Journal of The Surface Finishing Society of Japan, 48, 12, 1225-1226 (1997).

Y. Matsumoto, Y. Ishikawa, M. Nishida and S. Ii
"A New Electrochemical Method to Prepare Mesoporous Titanium(IV) Oxide Photocatalyst Fixed on Alumite Substrate"
The Journal of Physical Chemistry B, 104, 17, 4204-4209 (2000).

Chapter 3 Electrodeposition of TiO_2 photocatalyst into Nano-Porous of Hard Alumite

The mechanism of TiO_2 one-step electrodeposition into the pores of hard alumite is discussed. The characterization and the photocatalytic activity of deposited TiO_2 are described. The structure of the prepared hard alumite fixed with TiO_2 is discussed. The content of this chapter is based on the following published paper:

Y. Ishikawa and Y. Matsumoto
"Electrodeposition of TiO_2 photocatalyst into Nano-Porous of Hard Alumite"
Electrochimica Acta, 46, 2819-2824 (2001).

Chapter 4 Preparation of Titanium(IV) Oxide Film on a Hard Alumite Substrate

The two deposition mechanisms of TiO_2 are discussed. The characterization and the photoatalytic activity of precipitated TiO_2 on hard alumite are described. The structure of the prepared hard alumite fixed with TiO_2 is discussed. The content of this

chapter is based on the following published paper:

Y. Ishikawa, Y. Hayashi and Y. Matsumoto

"Preparation of Titanium(IV) Oxide Film on a Hard Alumite Substrate"

Journal of Materials Research, 17, 9, 2373-2378 (2002).

Chapter 5 Electrodeposition of TiO_2 into Porous Alumite Prepared in Phosphoric Acid

The mechanism of TiO_2 one-step electrodeposition into the pores of alumite prepared in phosophoric acid is discussed. The characterization and the photocatalytic activity of deposited TiO_2 are described. The structure of the prepared alumite fixed with TiO_2 is discussed. The content of this chapter is based on the following paper:

Y. Ishikawa and Y. Matsumoto

"Electrodeposition of TiO_2 into Porous Alumite Prepared in Phosphoric Acid"

Solid State Ionics, 151, 213-218 (2002).

Part II: Surface treatment of inorganic materials using TiO_2 photocatalytic reaction.

Chapter 6 Surface Treatment of SiC and Diamond Using Titanium(IV) Oxide Photocatalyst

The TiO_2 photocatalytic oxidation of silicon carbide and diamond surfaces is demonstrated. The mechanism of the photoatalytic reaction is discussed. The content of this chapter is based on the following paper.

Y. Matsumoto and Y. Ishikawa

"Surface Treatment of Diamond and Silicon Carbide Using Titanium Dioxide" Proceeding of the 19th Korea-Japan International Seminar on Ceramics, 295-298 (2002)

Chapter 7 General Conclusion

In this chapter, the general conclusions of present thesis are described.

ACKNOWLEDGEMENTS

I wish to express my sincerest thanks to Prof. Yasumichi Matsumoto for his invaluable comments and suggestions, and his encouragement through the period of this study. I am also grateful to the committee members of my research, Prof. Chuichi Hirayama and Prof. Tsutomu Hirose. Thanks are also due to the staff of the Matsumoto Laboratory, Dr. Michio Koinuma and Mr. Kai Kamada for their encouragement and helpful suggestions.

I gratefully acknowledge Prof. Minoru Nishida, for TEM work and helpful comments. It is also a pleasure for me to thank Prof. Junji Watanabe for his encouragement, useful discussions and kindly giving SiC and diamond substrates.

I am deeply thankful to Mr. Koji Nakashimam Ms. Seiko Sakaki, Mr. Junichi Ozawa, Ms. Ryoko Kabayama, Ms. Yoko Nishida, Mr. Yasunori Hayashi and Mr. Shinichi Taniguchi for their encouragement and assistance. I am grateful to Ms. Kiyomi Tahara, Secretary in this laboratory, for her assistance.

I am also thankful to Sasakawa Scientific Research Grant from The Japan Science Society and Sagawa Foundation for Promotion of Frontier Science and Japan Society for the Promotion of Science for the supports.

Finally, I sincerely thank my parents for their support and hearty encouragement through my student life.

Yoshie ISHIKAWA

Kumamoto

March, 2003

Chapter 1

Introduction

1. 1 General Background

In 1972, Honda and Fujishima reported the early work on photoelectrochemical reaction at semiconducting TiO_2 electrode. They discovered the evolution of oxygen on TiO_2 electrode surface and that of hydrogen on platinum opposite electrode surface as shown in Fig. 1. 1, when the surface of the TiO_2 electrode was illuminated. This phenomenon is referred to as the Honda-Fujishima effect and attracted the attention due to the conversion of light energy to electrical energy.[1] Solar cells using the Honda-Fujishima effect have been investigated. Especially, Ru-based dye sensitized solar cell, which reported by Grätzel et al. in 1991 and referred to as the Grätzel cell, has been attracted the attention, because of the high energy efficiency of which.[2] The oxidative decomposition of various organic compounds by active oxygen species generated on illuminated TiO_2 surface has been also reported by numerous investigators. The applications of the strong oxidative activity of TiO_2 photocatalysis to the antibacterial action and the decomposition of harmful compounds such as environmental endocrine disrupters in atmosphere, water, and soil have been developed. Therefore, the various commercial products added the TiO_2 photocatalytic function have been developed such as an air and water purifier, and air conditioner. Moreover, the surface of illuminated TiO_2 shows superhydrophilicity. This phenomenon is applied to the function of the fog proof and the self-cleaning by the combination with the high oxidative activity of the TiO_2 as stated above.[1] Consequently, the TiO_2 photocatalyst shows various useful advantages and have been investigated in various active areas. The practical applications of TiO_2 photocatalysis are shown in Table 1.

1. 2 TiO_2 photocatalyst

1. 2. 1 The principle of TiO_2 photocatalysis

Semiconductors can act as sensitizers for light-reduced redox processes due to their electronic structure, which is characterized by a filled valence band and an empty conduction band. Among the several semiconductor materials tested for photocatalysis, TiO_2 has proved to be the best one due to its strong oxidizing power under UV illumination and its chemical stability.

When a photon with an energy of hv matches or exceeds the bandgap energy of TiO_2 (ca. 3.0 eV) an electron, e_{cb}^-, is promoted from the valence band into the conduction band leaving a hole, h_{vb}^+ behind (eq 1). Excited state conductionband electrons and valence band holes can recombine and dissipate the input energy as heat, get trapped in metastable surface states, or react with electron donors and electron acceptors adsorbed on the TiO_2 surface or within the surrounding electrical double layer of the charged particles as shown in Fig. 1. 2. When water and O_2 are adsorbed on TiO_2 surface, active oxygen species such as hydroxyl radicals ($OH^\cdot$) and superoxide radical anion ($O_2^{\cdot -}$) or hydroperoxyl radical ($HO_2^\cdot$) generate (eq 2-4).[3]

$TiO_2 \rightarrow e_{cb}^- + h_{vb}^+$ (1)

$H_2O + h^+ \rightarrow OH^\cdot + H^+$ (2)

$O_2 + e^- \rightarrow O_2^{\cdot -}$ (3)

$O_2^{\cdot -} + H^+ \leftrightarrow HO_2^\cdot$ (4)

In particular, the hydroxyl radical, which have strong oxidizing power, can react with most organic compounds and decompose to CO_2. Therefore, useful phenomenon such as antibacterial action and decomposition of toxic in atmosphere, water and soil appear on surface of illuminated TiO_2.

1. 2. 2 Preparation and Fixation of TiO_2

Various preparation methods for the TiO_2 photocatalyst have been reported to date such as sol-gel method, CVD method and PVD method. In particular, the sol-gel or a similar method is the most important,[5-15] because the prepared TiO_2 has a small size and therefore, high specific surface area which is preferable for the catalyst.[13,16] In many of these methods, heat-treatment is generally necessary for the crystallization of anatase to produce a high photocatalytic activity.[10-12,14-16] Thus, meso-porous and/or nano-sized TiO_2 with the anatase structure is very useful for the photocatalysis, although the cost for the preparation of these types of TiO_2 is generally high. On the other hand, from the point of view of practical use, the fixation of the TiO_2 photocatalyst onto a substrate is also very important, and some methods to fix the TiO_2 photocatalyst onto some substrates have been developed.[18-24]

1. 3 Aims of the present study

Part I: Preparation of TiO_2 photocatalyst film on alumite substrate. (Chapter 2-5)

The development of a low-cost preparation and fixation of the TiO_2 photocatalyst is necessary for practical use. The soft solution process (SSP) is very important for the preparation of advanced inorganic materials such as hydroxyapatite, perovskite-type oxides and spinel-type oxide.[25-32] These low-cost processes have been used under environmentally benign conditions. Therefore, the SSP will be very important process for practical use. This study deals with the SSP for the preparation and fixation of the TiO_2 photocatalyst.

Aluminum is widely used as a building material, because it is relatively cheap and light. Generally, aluminum is electrochemically oxidized to produce an alumite (aluminum with a porous alumina film, denoted by Al/Al_2O_3), which protects against corrosion.[33,34] It is well known that the alumite prepared by anodic oxidation in sulfuric

and phosphoric acids has self-organized and nano-sized pores.[33-36] Some metal and metal oxides can be deposited in the pores of the alumina film by ac and/or dc electrolysis, and some metal deposited alumite is used as 'colored alumite'.[33,37] Alumite will be useful as a substrate for the TiO_2 photocatalyst film, because the alumite has nano-micro-sized pores and may act as a carrier of the catalyst.

Part II: Surface treatment of inorganic materials using TiO_2 photocatalytic reaction. (Chapter 6)

TiO_2 is a famous photocatalyst that decomposes various organic compounds under illumination as stated above.[38-45] In particular, Tatsuma et al.[46] recently reported the photocatalytic decomposition of organic solid materials such as a polystyrene and polyethylene using a TiO_2 photocatalyst. During the photocatalytic process, the OH radical and/or other activated oxygen species on the surface act as oxidizing agents, and will also act as oxidizing agents to oxidize inorganic solid materials; solid sulfur is oxidized to the sulfate ion by the TiO_2 photocatalysis.[47] This result suggests that TiO_2 may act as a photocatalyst to oxidize and decompose other inorganic solid materials. In chapter 6, a new surface treatment of inorganic materials such as SiC and diamond using a TiO_2 photocatalyst under mild conditions is demonstrated.

References

(1) Fujishima, A.; Hashimoto, K; Watanabe, T. *TiO_2 Photocatalysis*; BKC: Japan, 1999.

(2) O'Regan, B.; Grätzel, M *Nature* **1991,** 353, 737.

(3) Hoffman, M. R; Martin, S. T.; Choi, W.; Bahnemann, D. W. *Chem. Rev.* **1995,** 95, 69-96.

(4) Hanley, T. L.; Luca, V.; Pickering, I.; Howe, R. F. *J. Phys. Chem. B* **2002,** 106, 1153-1160.

(5) Kaviratna, P. D.; Peden, C. H. F. *Heterogeneous Hydrocarbon Oxidation*; American Chemical Society: Washington DC, 1996.

(6) Wong, J. C. S.; Linsebigler, A.; Lu, G.; Fan, J.; Yates, Jr. J. T. *J. Phys. Chem.* **1995,** 99, 335.

(7) Goren, Z.; Willner, I.; Nelson, A. J.; Frank, A. J. *J. Phys. Chem.* **1990,** 94, 3784.

(8) Aritani, H.; Akasaka, N.; Tanaka, T.; Funabiki, T.; Yoshida, S.; Gotoh, H.; Okamoto, Y. *J. Chem. Soc., Faraday Trans.* **1996,** 92, 2625.

(9) Sopyan, I.; Watanabe, M.; Murasawa, S.; Hashimoto, K.; Fujishima, A. *J. Photochem. Photobiol. A: Chem.* **1996,** 98, 79.

(10) Negishi, N.; Iyoda, T.; Hashimoto, K.; Fujishima, A. *Chem. Lett.* **1995,** 841.

(11) Hashimoto, K.; Fujishima, A. *TiO_2 photocatalysis*; CMC: Tokyo, 1998.

(12) Kominami, H.; Matsuura, T.; Iwai, K.; Ohtani, B.; Nishimoto, S.; Kera, Y. *Chem. Lett.* **1995,** 693.

(13) Dagan, G.; Tomikiewicz, M. *J. Phys. Chem.* **1993,** 97, 12651.

(14) Sclafani, A.; Palmisano, L.; Schiavello, M. *J. Phys. Chem.* **1990,** 94, 829.

(15) Ohtani, B.; Bowman, R. M.; Colombo, Jr. D. P.; Kominami, H.; Noguchi, H.; Uosaki, K. *Chem. Lett.* **1998,** 579.

(16) Ohtani, B.; Ogawa, Y.; Nishimoto, S. *J. Phys. Chem, B.* **1997,** 101, 3746.

(17) Anpo, M; Aikawa, N.; Kubokawa, Y.; Che, M.; Louis, C.; Giamello, E. *J. Phys.*

Chem, **1985,** 89, 5017.

(18) Jackson, N. B.; Wang, C. M.; Luo, Z.; Schwitzgebel, J.; Ekerdt, J. G.; Brock, J. R.;Heller, A. *J. Electrochem. Soc.* **1991,** 138, 3660.

(19) Matsubara, H.; Takada, M.; Koyama, S.; Hashimoto, K.; Fujishima, A. *Chem. Lett.* **1995,** 767.

(20) Deki, S.; Aoi, Y.; Hiroi, O.; Kajinami, A. *Chem. Lett.* **1996,** 433.

(21) Miyoshi, H.; Nippa, S.; Uchida, H.; Mori, H.; Yoneyama, H. *Bull. Chem. Soc. Jpn.* **1990,** 63, 3380.

(22) Ikeda, K.; Sakai, H.; Baba, R.; Hashimoto, K.; Fujishima, A. *J. Phys. Chem, B.* **1997,** 101, 2617.

(23) Watanabe, T.; Kitamura, A.; Kojima, E.; Nakayama, C.; Hashimoto, K.; Fujishima, A. *Photocatalytic Purification and Treatment of Water and Air*; Elsevier Science Publishers B. V.: Amsterdam, 1993.

(24) Kavan, L.; O'Regan, B.; Kay, A.; Grätzel, M. *J. Electroanal. Chem.* **1993,** 346, 291.

(25) Yoo, S. –E.; Hayashi, M.; Ishizawa, N.; Yoshimura, M. *J. Am. Ceram. Soc.* **1990,** 73, 2561

(26) Kajiyoshi, K.; Tomono, K.; Hamaji, Y.; Kasanami, T.; Yoshimura, M. *J. Am. Ceram. Soc.* **1994,** 77, 2889.

(27) Konno, H.; Tokita, M.; Furuichi, R. *J. Electrochem. Soc.* **1990,** 137, 361.

(28) Sasaki, T.; Morikawa, T.; Hombo, J.; Matsumoto, Y. *Denki Kagaku* **1990,** 58, 567.

(29) Matsumoto, Y.; Sasaki, T.; Hombo, J. *Inorg. Chem.* **1992,** 31, 738.

(30) Matsumoto, Y.; Adachi, H.; Hombo, J. *Electrochim. Acta* **1993,** 38, 1145.

(31) Matsumoto, Y.; Adachi, H.; Hombo, J. *J. Am. Ceram. Soc.* **1993,** 76, 769.

(32) Matsumoto, Y.; Hombo, J.; Qiong, C. *J. Electroanal. Chem.* **1990,** 279, 331.

(33) Mita, I.; Kuroda, K.; Suzuki, K.; Muramatsu, Y.; Nemoto, S.; Yamada, M. *Handbook of Aluminum Surface Treatment*; Light Metal Publishing, Tokyo, 1980.

(34) Sato, T. *Trans. Inst. Met. Finish.* **1982,** 60, 25.

(35) Li, A. P.; Müller, F.; Birner, A.; Nielsch, K.; Gösele, U. *J. Appl. Phys.* **1998,** 84, 6023.

(36) Masuda, H.; Hasegawa, F.; Ono, S. *J. Electrochem. Soc.* **1997,** 144, 127.

(37) Sato, T.; Sakai, S. *Trans. Inst. Met. Finish.* **1979,** 57, 43.

(38) Fujishima, A.; Honda, K. *Nature* **1972,** 238, 37.

(39) Jaeger, C. D.; Bard, A. J. *J. Phys. Chem.* **1979,** 83, 3146.

(40) Sato, S.; White, J. M. *Chem. Phys. Lett.* **1980,** 72, 83.

(41) Inoue, T.; Fujishima, A.; Konishi, S.; Honda, K. *Nature* **1979,** 277, 637.

(42) Wong, J. C. S.; Linsebigler, A.; Lu, G.; Fan, J.; Yates, J. T., Jr. *J. Phys. Chem.* **1995,** 99, 335.

(43) Goren, Z.; Willner, I.; Nelson, A. J.; Frank, A. J. *J. Phys. Chem.* **1990,** 94, 3784.

(44) Sopyan, I.; Watanabe, M.; Murasawa, S.; Hashimito, K.; Fujishima, A. *J. Photochem. Photobiol. A* **1996,** 98, 79.

(45) Nozik, A. J.; Memming, R. *J. Phys. Chem.* **1996,** 100, 13061.

(46) Tatsuma, T.; Tachibana, S.; Fujishima, A. *J. Phys. Chem. B* **2001,** 105, 6987.

(47) Matsumoto, Y.; Nagai, H.; Sato, E. *J. Phys. Chem.* **1982,** 86, 4664.

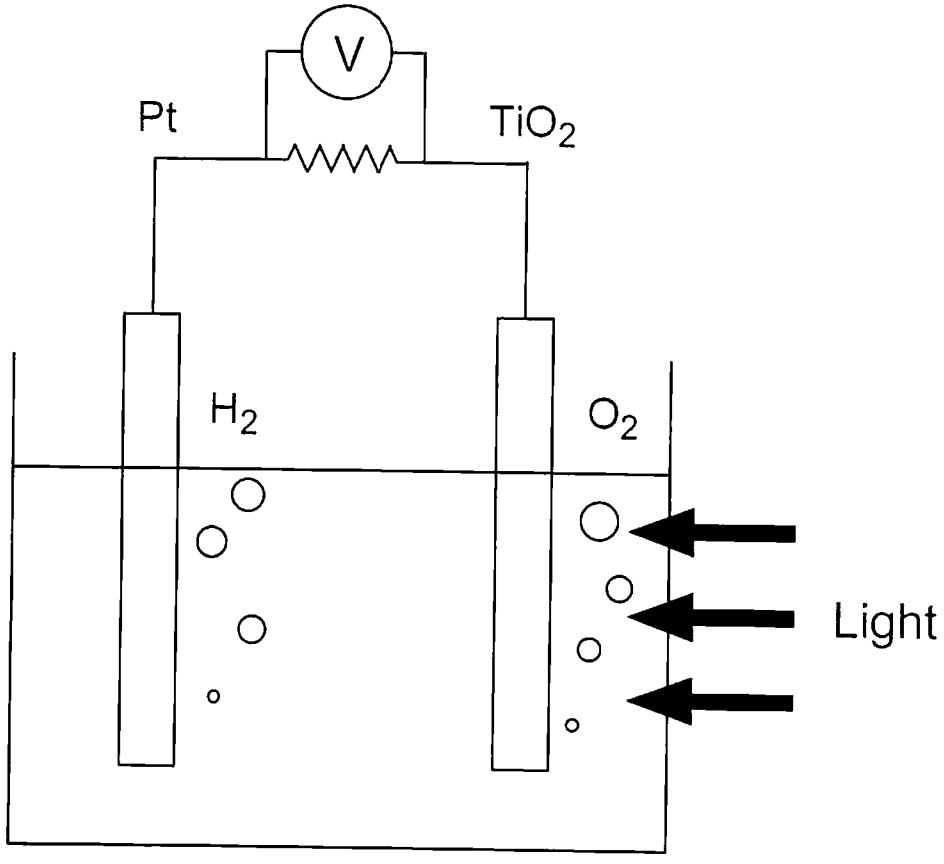

Fig. 1. 1. Water photolysis by TiO_2 electrode system.

Table 1 The practical application of TiO_2 photocatalysis.

Application	Principle	Specific examples
solar cell	conversion of light energy to electrical energy	Grätzel cell
antibacterial	oxidation-reduction reaction on surface	antibacterial tiles
decomposition of pollutants	oxidation-reduction reaction on surface	water purifier air purifier air conditioner
anti fog	superhydrophilicity	anti fogging mirror
self-cleaning	oxidation-reduction reaction on surface + superhydrophilicity	building materials coating materials

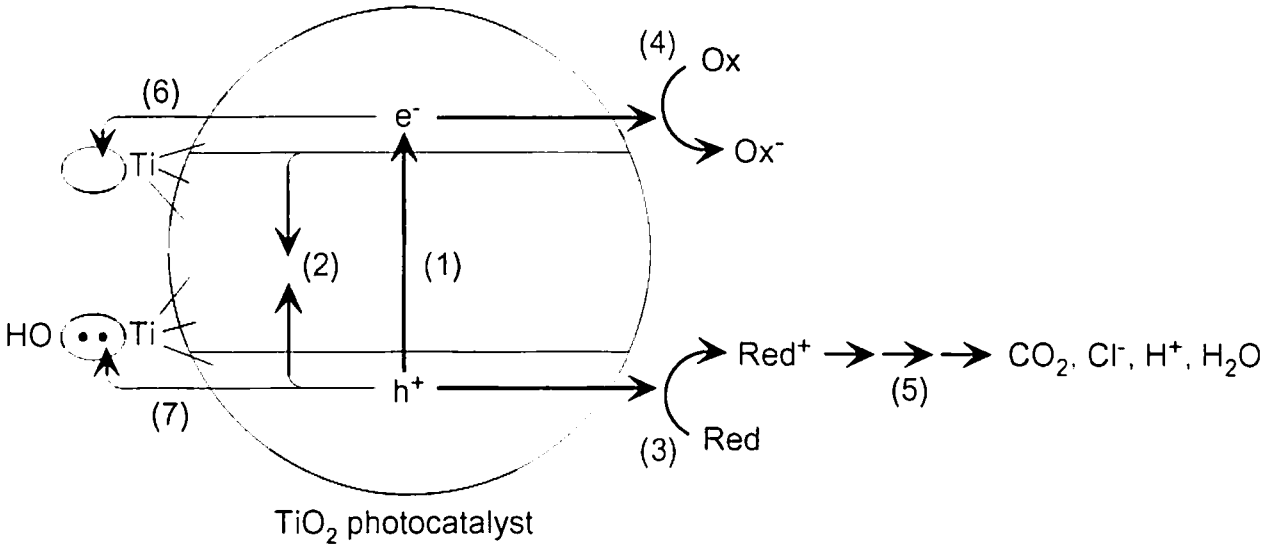

Fig. 1. 2. Primary steps in the photoelectrochemical mechanism: (1) formation of charge carriers by a photon; (2) charge carrier recombination to liberate heat; (3) initiation of an oxidative pathway by a valence band hole; (4) initiation of a reductive pathway by a conduction band electron; (5) further thermal and photocatalytic reactions to yield mineralization products; (6) trapping of a conduction band electron in a dangling surficial bond to yield Ti(III); (7) trapping of a valence-band hole at a surficial titanol group.

Chapter 2

A New Electrocheical Method to Prepare Mesoporous Titanium(IV) Oxide Photocatalyst Fixed on Alumite Substrate

2. 1 Introduction

We developed a new electrochemical method to prepare the TiO_2 photocatalyst and to directly fix it onto Al/Al_2O_3 alumite substrate directly with low cost, which is usually used as a cheap building material. The electrolysis was carried out at 50-90 °C, and no heat-treatment was necessary for the deposited TiO_2, because the as-deposited TiO_2 had already been crystallized. In this study, a new electrochemical method consisting of a two-step electrolysis and the characterization of the deposited TiO_2 film are described, and the deposition mechanism is discussed. Moreover, the high catalytic activity of the prepared $Al/Al_2O_3/TiO_2$ plate for the decomposition of acetaldehyde is demonstrated, and its mechanism is also discussed.

2. 2 Experimental

An aluminum plate (60 x 50 mm, thickness: 2 mm) was etched by immersion in alkaline solution and then electrochemically oxidized at 10 mA/cm^2 in H_2SO_4 solution (1.8 M) for 25 min to prepare the porous alumite on its surface. The radii of the pores were about 10 nm.[1] The aluminum substrate coated with porous alumite by the previous method was coated with the TiO_2 film by the following two electrolysis steps: First, the electrolysis was carried out in a mixed aqueous solution consisting of 10^{-2} M $(NH_4)TiO(C_2O_4)$ and 2.5 x 10^{-3} M $(COOH)_2$ adjusted to pH 4 by titration with NH_4OH, under an a.c. bias of 8 V for 10 min at 50 °C. The graphite plate (50 x 60 mm) was used as the counter electrode, and the distance between the counter and working electrodes was fixed at 50 mm. The a.c. current density was in the range from 20 mA/cm^2 (at initial

electrolysis time) to 7 mA/cm^2 (at final electrolysis time). In this stage, a thin TiO_2 film (denoted by TO-1) was uniformly deposited on the substrate, but scarcely showed photocatalytic activity as stated in a later section. In the subsequent electrolysis step, the TiO_2 deposited aluminum substrate was again electrochemically oxidized in 1.23 x 10^{-2} M $TiCl_3$ solution adjusted to pH 3 by titration with NH_4OH. In this case, pulse electrolysis with a constant current of 1.7 mA/cm^2 for a 5 x 10^{-2} s cycle with a 10^{-2} s interval was carried out at 80-90 °C. The pulse bias voltage was about 0.5 V. Consequently, the alumite was uniformly and completely coated with the deposited TiO_2 film (denoted by TO-2) by the present two-step electrolysis. The TO-1 and TO-2 are denoted as AOT in this paper.

The morphology and the elemental distribution of the AOT plates were observed using electron probe microanalysis (EPMA). The amount of the deposited TiO_2 in the TO-2 was 0.02 g/30 cm^2 based on analysis by inductively coupled plasma (ICP) spectroscopy, where the AOT was dissolved with 1.2 M H_2SO_4 and then the solution was analyzed. The crystal structure and the morphology of the prepared TiO_2 were analyzed by electron diffraction, Raman spectroscopy, and transmission electron microscopy (TEM), since no diffraction peak was observed in the X-ray diffraction pattern. The UV and visible absorption spectrum of the coated TiO_2 was measured by a UV/VIS spectrophotometer. Anatase (99.9 %, Wako, Ltd.), rutile (99.9 %, Wako, Ltd.) and amorphous TiO_2 (99.9 %, Wako, Ltd.) powders were used as the standard sample in order to estimate the weight ratio of anatase and rutile in the prepared TO-2 sample during the Raman measurement.

The photocatalytic activity of the AOT plate was measured for the photo-decomposition of acetaldehyde. A small amount of acetaldehyde gas was injected into a 1000 ml cylindrical quartz cell (62.5 cm^2 x 16 cm, the concentration was about 10 ppm), where the AOT plate was fixed in the cell in advance, and then illuminated. A 500 W

xenon lamp (200 mW/cm^2) and a 24 W fluorescent lamp (rare-earth lamp, Mitsubishi-BS3601B, 10 mW/cm^2) were used as the light sources. The variation in the concentration of acetaldehyde and the produced CO_2 were measured using gas chromatography. The humidity in the reactor cell was 20-30 percent at 30 °C unless otherwise stated. The P-25 TiO_2 (Degussa, 30 nm average particle size, 50 m^2/g BET surface area), anatase (0.30 μm average particle size, as stated above) and rutile (0.30 μm average particle size, as stated above) powders were also used as photocatalysts for comparison of the photocatalytic activity.

2. 3 Results and Discussion

2. 3. 1 Morphology of the AOT.

The electrodeposition of the TO-1 by a.c. electrolysis will occur in the pores of the alumite as follows:

$$(NH_4)_2[TiO(C_2O_4)_2] \rightarrow TiO(C_2O_4)_2^{2-} + 2NH_4^+ \quad (1)$$

$$2H_2O + 2e^- \rightarrow H_2 \text{ (and/or } 2H_{ads}) + 2OH^- \quad (2)$$

$$TiO(C_2O_4)_2^{2-} + 2OH^- \rightarrow TiO_2 + H_2O + 2(C_2O_4)^{2-} \quad (3)$$

$(NH_4)_2[TiO(C_2O_4)_2]$ will dissolve and then dissociate into $TiO(C_2O_4)_2^{2-}$ and ammonium ions (Eq. (1)) in aqueous solution before the electrolysis. Cathodic bias during the a.c. electrolysis brings about the electrochemical reaction (2) where OH^- ion is produced. Finally, TiO_2 (which will be somewhat hydrated) was produced in the pores of the alumite (Eq. (3)). The reaction model is illustrated in (a) of Fig. 2. 1. The above reactions were confirmed by the following experimental results. TiO_2 was precipitated in the solution when the pH of the solution containing $(NH_4)_2[TiO(C_2O_4)_2]$ was adjusted to about 5 from 4 by titration of the NH_4OH solution. Moreover, TiO_2 was deposited onto a Pt electrode by cathodic bias during d.c. electrolysis in the $(NH_4)_2[TiO(C_2O_4)_2]$ aqueous solution, but not anodic bias. Nevertheless, the a.c. electrolysis was necessary

for the deposition of the TiO_2 in the pores of the alumite. Probably, the diffusion of $TiO(C_2O_4)_2^{2-}$ in to the pores of alumite will totally increase under the a.c. bias, leading to the deposition of the TiO_2 in the pores in alumite as is well known.[2]

Figure 2. 2 shows the line profile of the EPMA elemental distribution in the cross section of the $Al/Al_2O_3/TiO_2$ interface in the TO-1 sample. The part where Al overlaps with O in the distribution corresponds to the alumite layer. Consequently, the TiO_2 exists in the bottom of the pores of the alumite as shown in the model. The amount of the deposited TiO_2 in the TO-1 was 0.6 mg/30 cm^2 according to the analysis by ICP spectroscopy.

The electrodeposition for the TO-2 will proceed on the surface of the TO-1 sample as follows:[3,4]

$$Ti^{3+} + H_2O \rightarrow TiOH^{2+} + H^+ \quad (4)$$

$$TiOH^{2+} \rightarrow e^- + \text{Ti (IV) oxo-species} \rightarrow TiO_2 \quad (5)$$

$TiOH^{2+}$ will be produced by the hydrolysis of Ti^{3+} in the diluting and pH adjusting processes of the $TiCl_3$ solution as described in the experimental section (Eq. (4)). $TiOH^{2+}$ will then be oxidized to Ti(IV) oxo-species (Eq. (4)) during the d.c. anodic pulse electrolysis. According to Kavan et al.[3,4] the Ti (IV) oxo-species is an intermediate between TiO^{2+} and TiO_2, consisting of partly dehydrated polymeric Ti (IV) hydroxide, which will be finally converted into TiO_2 by dehydration during the present electrolysis. This reaction model is illustrated in (b) of Fig. 2. 1.

Figure 2. 3 shows the line profile of the EPMA elemental distribution in the cross section of the TO-2 and its expected model. The TiO_2 layer produced in the above reactions uniformly covered the alumite surface and its thickness was about 6-7 μm. The amount of the TiO_2 in the TO-2 was much larger than that of the TO-1 and was about 0.02 g/30 cm^2 according to the ICP analysis.

Consequently, the uniform thick TiO_2 layer was fixed on the alumite surface in the TO-

2. Both these steps consisting of the a.c. and d.c. electrolyses were very important for the TiO_2 fixation, because the deposited TiO_2 was not uniform and did not adhere to the alumite when only the pulse d.c. electrolysis was directly made on the alumite without the a.c. electrolysis. Some polymerized TiO_2 probably existing in the pores of the TO-1 will combine with the Ti (IV) oxo-species prepared during the subsequent pulse d.c. electrolysis, thus leading to the strong fixation of the TiO_2 layer in the TO-2.

2. 3. 2 Characterization of the AOT.

The as-deposited TiO_2 in the TO-2 was X-ray amorphous, but consisted of a mixed phase of the anatase and rutile structures according to the Raman spectroscopy measurements as shown in Fig. 2. 4.[5-7] Figure 2. 5 (a) shows a TEM image of the TiO_2 in the TO-2. It was found from this figure that the particle sizes of the TiO_2 were in the range from 4 to 5 nm. Numerous stripes were also observed suggesting that many crystallized particles were contained in the TO-2. According to the electron diffraction pattern analysis shown in Fig. 2. 5 (b), the TiO_2 consisted of the anatase, rutile, and amorphous phases. This result is in agreement with that of the Raman results.

On the other hand, the TO-1 consisted of the amorphous phase of TiO_2, because no Raman peak was observed (In this measurement, a large amount of powder of the TO-1 films which corresponds to >0.006 g/30 cm^2 as TiO_2, was used as the test sample. The powder was collected by mechanical release from many TO-1 samples). In fact, no Raman peak was observed for the amorphous TiO_2 powder. The morphological difference between the TO-1 and TO-2 samples will be mainly based on the electrolysis temperature. The TiO_2 in the TO-2 sample was amorphous and scarcely showed any photocatalytic activity, when the second pulse d.c. electrolysis was carried out at room temperature. However, the TiO_2 was crystallized into the mixed phase of anatase and rutile and showed the catalytic activity when this TO-2 sample was heat-treated at 500

°C. Therefore, we tried to prepare the crystallized TO-1 sample by a.c. electrolysis at 90 °C. The adhesion of the TiO_2, however, was not good under this condition. Consequently, the TO-2 sample prepared under the present conditions was the best from the point of view of uniform deposition, the adhesion and the photocatalysis.

The weight ratio of the anatase/rutile phase in the TO-2 sample was estimated from the ratio of the Raman peak area for each phase as follows. Figure 2. 6 shows the variation in the Raman spectra of the mixture samples consisting of the anatase and rutile phases where A:R denotes the weight ratio of the anatase and rutile phases. Figure 2. 7 shows the ratio of the Raman peak area of the anatase phase at 143 cm^{-1} to that of the rutile phase at 440 cm^{-1} in Fig. 2. 6, as a function of the percentage of the anatase phase. It is estimated from Fig. 2. 7 that the weight ratio of the anatase/rutile phase is about one in the TO-2 sample.

The BET specific area of the TO-2 was about 140 m^2/g. The high specific area brought about by the nano-sized TiO_2 particles in the TO-2 is very useful for the photocatalytic reaction. Consequently, the present AOT is a unique plate coated with a meso-porous TiO_2 film consisting of nano-sized anatase, rutile particles and the amorphous phase.

The absorption spectrum of the as-deposited TiO_2 is shown in Fig. 2. 8. In this figure, spectra of the various TiO_2 samples are also shown for comparison. The TO-1 shows a blue shift in the spectrum. A similar phenomenon has been observed for the quantized TiO_2 particles and highly dispersed TiO_2 in the porous substrate.[8-11] Therefore, the blue shift in the TO-1 may be attributed to the amorphous and dispersed TiO_2 deposited into the pores of Al_2O_3. On the other hand, the TO-2 shows the useful spectrum similar to P-25 or anatase in the photocatalysis. In the case of the TO-2, a tailing absorbance in the visible region of 400-500 nm was observed. A similar absorbance has been observed for the TiO_2 produced by the hydrolysis of $TiCl_4$.[12]

Serpone suggested that the visible absorption is attributed to the charge transfer transition from Cl^- to Ti (IV).[12] The same phenomenon will occur in the visible absorption mechanism for the TO-2 sample, because the TO-2 is prepared in the $TiCl_3$ solution.

2. 3. 3 Photocatalytic Activity of the AOT.

Figure 2. 9 shows the concentration of acetaldehyde as a function of the illumination time of various light sources. In Fig. 2. 9 (a), a 500 W xenon lamp was used as the light source. The concentration immediately decreased by the illumination in the case of the TO-2, indicating that its photocatalytic activity for the decomposition of acetaldehyde is very high. The P-25 (0.02 g /30 cm^2) powder showed a similar photocatalytic activity, but not the TO-1. There are two reasons why the TO-1 sample shows only a slight photocatalytic activity. One is the very small amount of the deposited TiO_2, which is much lower than that in the TO-2 sample by two orders. The other is the amorphous phase of the TiO_2 in the TO-1 sample. The amorphous TiO_2, in general, does not have photocatalytic activity or have negligible activity.[13] Moreover, the blue shift in the absorption spectrum of the TO-1 sample shown in Fig. 2. 6 is undesirable for the photocatalysis under illumination using the present light sources.

In Fig. 2. 9 (b), a 24 W fluorescent lamp (F-lamp) was used as the light source. It is shown that the photocatalytic activity of the TO-2 is slightly more active than that of the P-25. Figure 2. 10 compares the specific photocatalytic activity per unit weight of the TiO_2 catalysts, where the initial concentration of acetaldehyde was 100 ppm because acetaldehyde was completely decomposed for some samples at 10 ppm. The amount of the decomposed acetaldehyde (per unit weight of the TiO_2 catalysts) after 1 h illuminate of 24 W fluorescent lamp was used as an indicator for the specific photocatalytic activity. The amorphous sample scarcely showed any photocatalytic activity. It is clear

that the activity of the TO-2 is more active than that of the P-25 especially under dry conditions. The high catalytic activity of the TO-2 sample will be mainly based on the nano-sized anatase particles prepared on the alumite, because the anatase TiO_2 used in this study shows a relatively high catalytic activity as shown in this figure.

In Fig. 2. 10, the effect of humidity on the photocatalytic decomposition of acetaldehyde is also shown. The high humidity condition decreased the photocatalytic activity for all the samples, and the effect was the strongest for the TO-2 in all the samples as shown in Fig. 2. 10. The effect of water vapor strongly depends on the concentration of the water vapor as well as the type and concentration of the organic compounds.[14-18] However, in general, the adsorbed water decreases the photocatalytic activity, except for the case of the extremely dilute concentration condition. One reason for the decreased effect is due to the competitive adsorption of water molecules on available hydroxyl adsorption site on the TiO_2 surface.[17,18]

Two mechanisms for the photocatalytic decomposition of organic compounds have been reported and depend on the type of organic compounds. One mechanism is the direct decomposition of the organic compounds by the produced hole in the valence band. The other is that of the indirect decomposition where some active species such as hydroxyl radical already produced by hole react with the organic compounds. It is not clear whether the present photo-decomposition of acetaldehyde proceeds by the former or the latter mechanism, although C. A. Jenkins and D. M. Murphy have reported that the acetaldehyde photo-decomposition proceeds by the former mechanism.[19] The products were analyzed using FT-IR and gas chromatography measurements. In the present test, the initial concentration of acetaldehyde was about 6290 ppm and 500 W xenon lamp was illuminated, since high concentrations of the products were necessary because of relatively low sensitivities of the FT-IR and gas chromatography analyses. About 6270 ppm of acetaldehyde was decomposed and CO_2 with the corresponding

concentration was detected in the cell after 45 min illumination, but no acetic acid on the surface of the TO-2 was found in the FT-IR analysis. Consequently, it was concluded that acetaldehyde was directly decomposed to CO_2 at the TO-2 sample under the present test conditions.

2. 4 Conclusions

In conclusion, a new preparation method has been developed using an electrochemical technique to prepare the meso-porous TiO_2 photocatalyst and to fix directly it onto the alumite substrate. It was found that the TiO_2 film consists of nano-sized particles with anatase, rutile and amorphous phases, and that its photocatalytic activity is very high for the decomposition of acetaldehyde. This new method will be very useful for the practical use of the photocatalyst, because the present electrochemical technique is very simple and inexpensive, and can be applied to cheap aluminum substrates with complex shapes and on a large scale.

Reference

(1) Bao, X.; Li, F.; Metzger, R. M. *J. Appl. Phys.* **1996,** 79, 4866.

(2) Sato, T.; Mita, K.; Kuroda, K.; Suzuki, K.; Muramatsu, Y.; Nemoto, S.; Yamada, M. *Handbook of Aluminium Surface Treatment*; Light Metal Publishing: Tokyo, 1980.

(3) Kavan, L.; O'Regan, B.; Kay, A.; Grätzel, M. *J. Electroanal. Chem.* **1993,** 346, 291.

(4) Rotzinger, F. P.; Grätzel, M. *Inorg. Chem.* **1987,** 26, 3704.

(5) Ocana, M.; Garcia-Ramos, J. V.; Serna, C. J. *J. Am. Ceram. Soc.*, **1992,** 75, 2010.

(6) Hsu, L. S.; Rujkorakarn. J. R. S.; She, C. Y. *J. Appl. Phys.* **1986,** 59, 3475.

(7) Zhang, M. S.; Yin, Z.; Chen, Q. *Ferroelectrics* **1995,** 168, 131.

(8) Liu, X; Lu K. K; Thomas J. K. *J. Chem. Soc. Faraday Trans.* **1993,** 89, 1861.

(9) Uchida, H.; Hirao, S.; Torimoto, T.; Kuwabata, S.; Sakata, T.; Mori, H.; Yoneyama, H. *Langmuir.* **1995,** 11, 3725.

(10) Domen, K.; Sakata, Y.; Kudo, A.; Maruya, K.; Onishi, T. *Bull. Chem. Soc. Jpn.* **1988,** 61, 359.

(11) Yamashita, H.; Ichihashi, Y.; Anpo, M.; Hashimoto, M.; Louis, C.; Che, M. *J. Phys. Chem.* **1996,** 100, 16041.

(12) Serpone, N.; Lawless, D.; Khairutdinov, R. *J. Phys. Chem.* **1995,** 99. 16646.

(13) Davidson, R. S.; Morrison, C. L.; Abraham, J. *J. Photochem.* **1984,** 24, 27.

(14) Jacoby, W. A.; Blake, D. M.; Noble, R. D.; Koval, C. A. *J. Catal.* **1995,** 157, 87.

(15) Suzuki, K. *Photocatalytic Purification and Treatment of Water and Air,* Elsevier Science Publishers B. V.: Amsterdam, 1993.

(16) Peral, J.; Ollis, D. F. *J. Catal.* **1992,** 136, 554.

(17) Fu, X.; Clark, L. A.; Zeltner, W. A.; Anderson, M. A. *J. Photochem. Photobiol. A: Chem.* **1996,** 97, 181.

(18) Fu, X.; Zeltner, W. A.; Anderson, M. A. *Semiconductor Nanoclusters Studies in Surface Science and Catalysis, Vol. 103,* Elsevier Science Publishers B. V.: Amsterdam, 1996.

(19) Jenkins, C. A.; Murphy, D. M. *J. Phys. Chem. B* **1999,** 103, 1019.

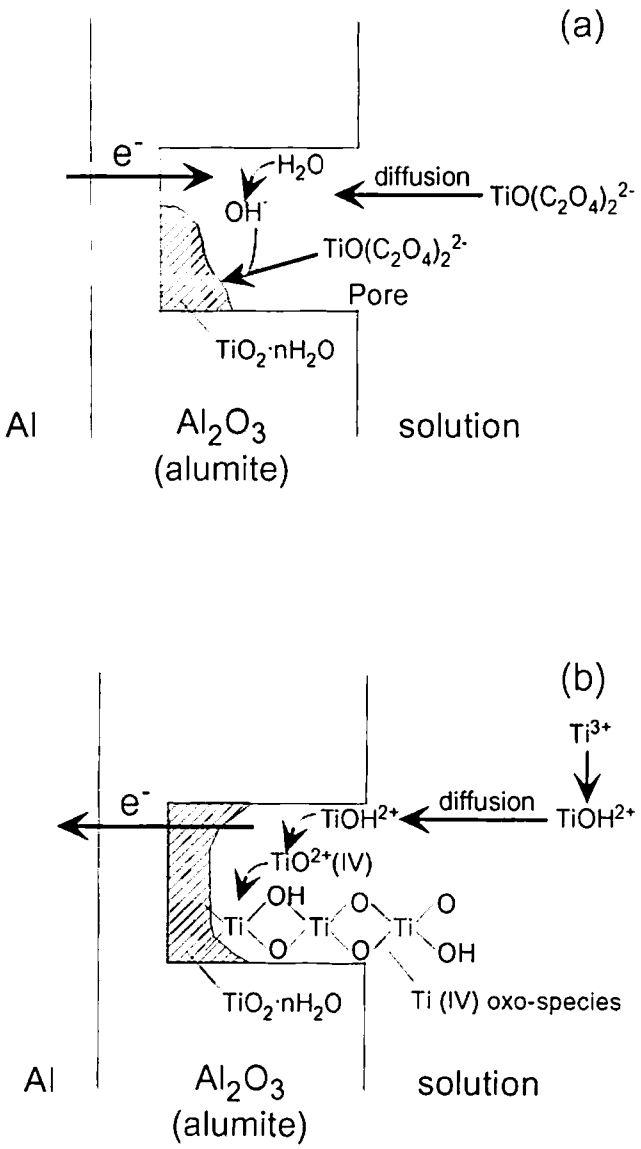

Fig. 2. 1. Models of the electrodeposition for the TO-1 (a) and TO-2 (b).

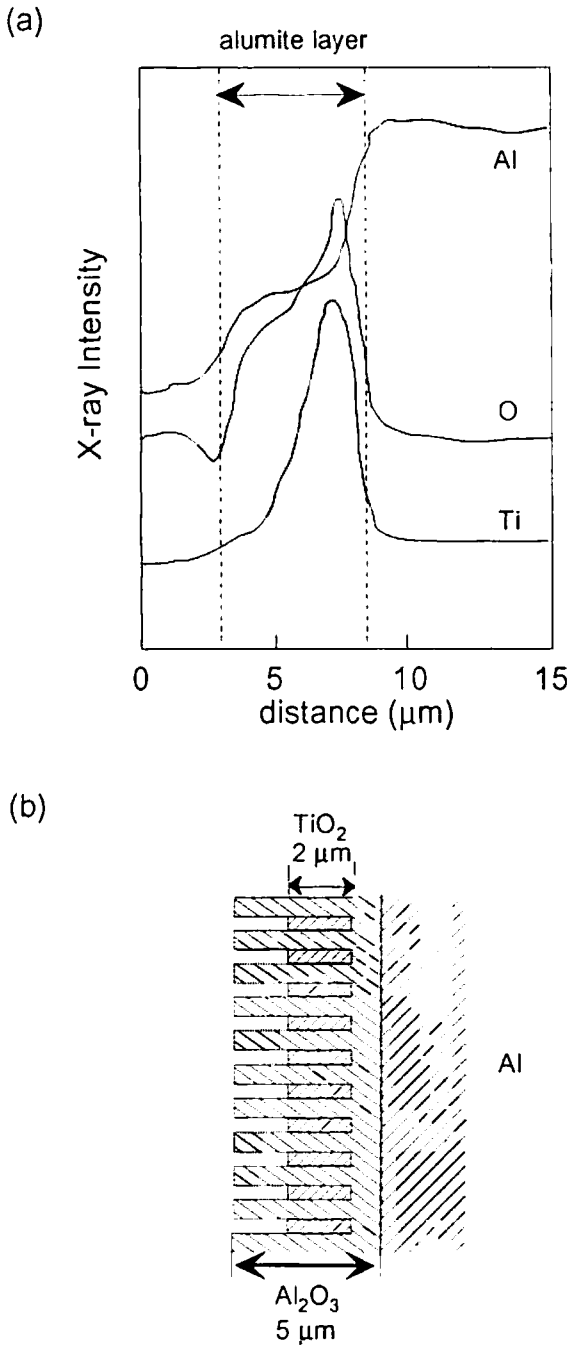

Fig. 2. 2. Line profile of the EPMA elemental distribution n the cross-section of the TO-1 sample (a) and its model (b).

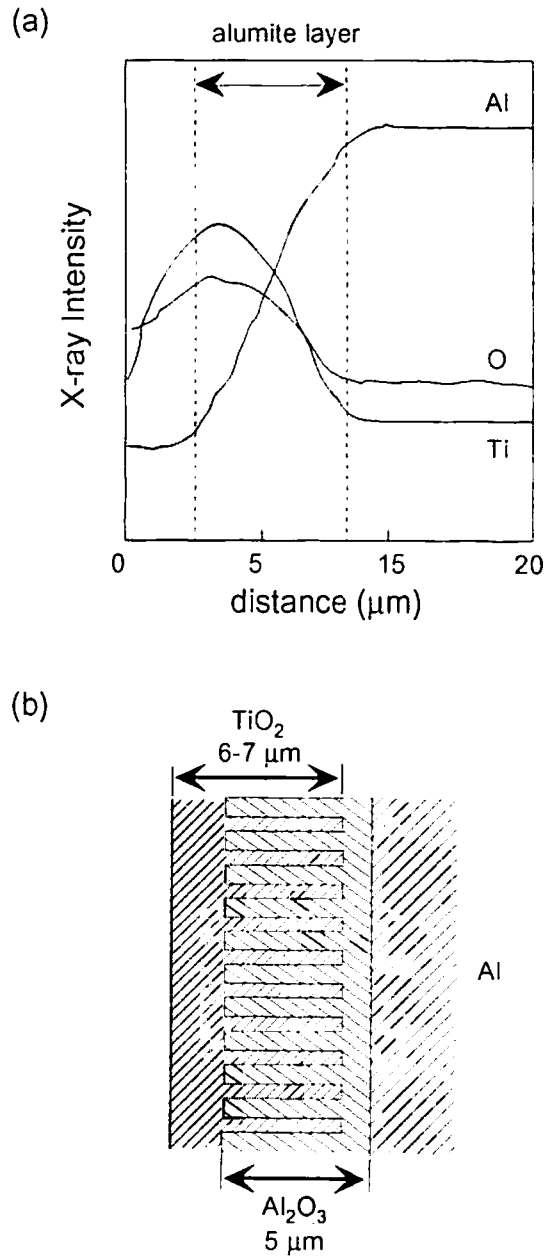

Fig. 2. 3. Line profile of the EPMA elemental distribution in the cross-section of the TO-2 sample (a) and its model (b).

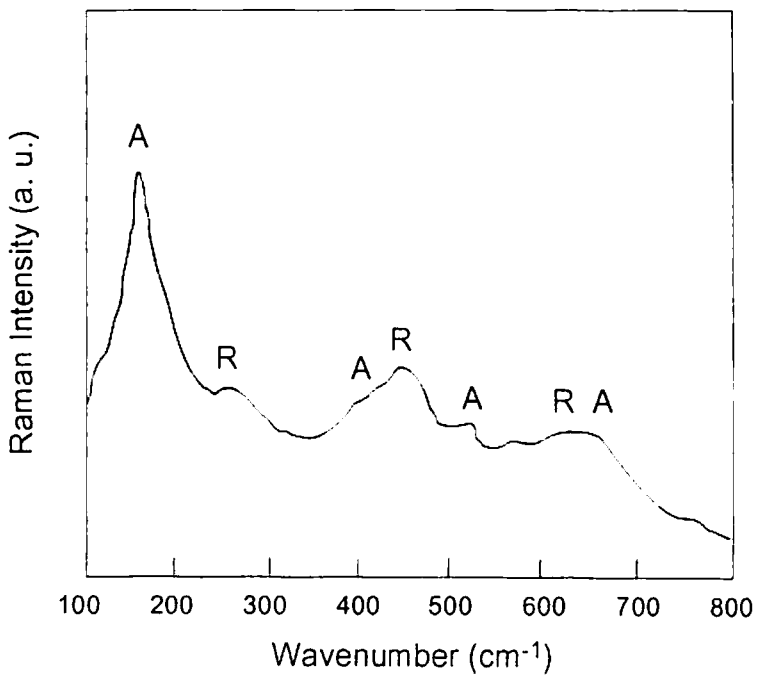

Fig. 2. 4. Raman spectrum of the deposited TiO_2 (TO-2). Peaks A and R correspond to the anatase and rutile phases, respectively.

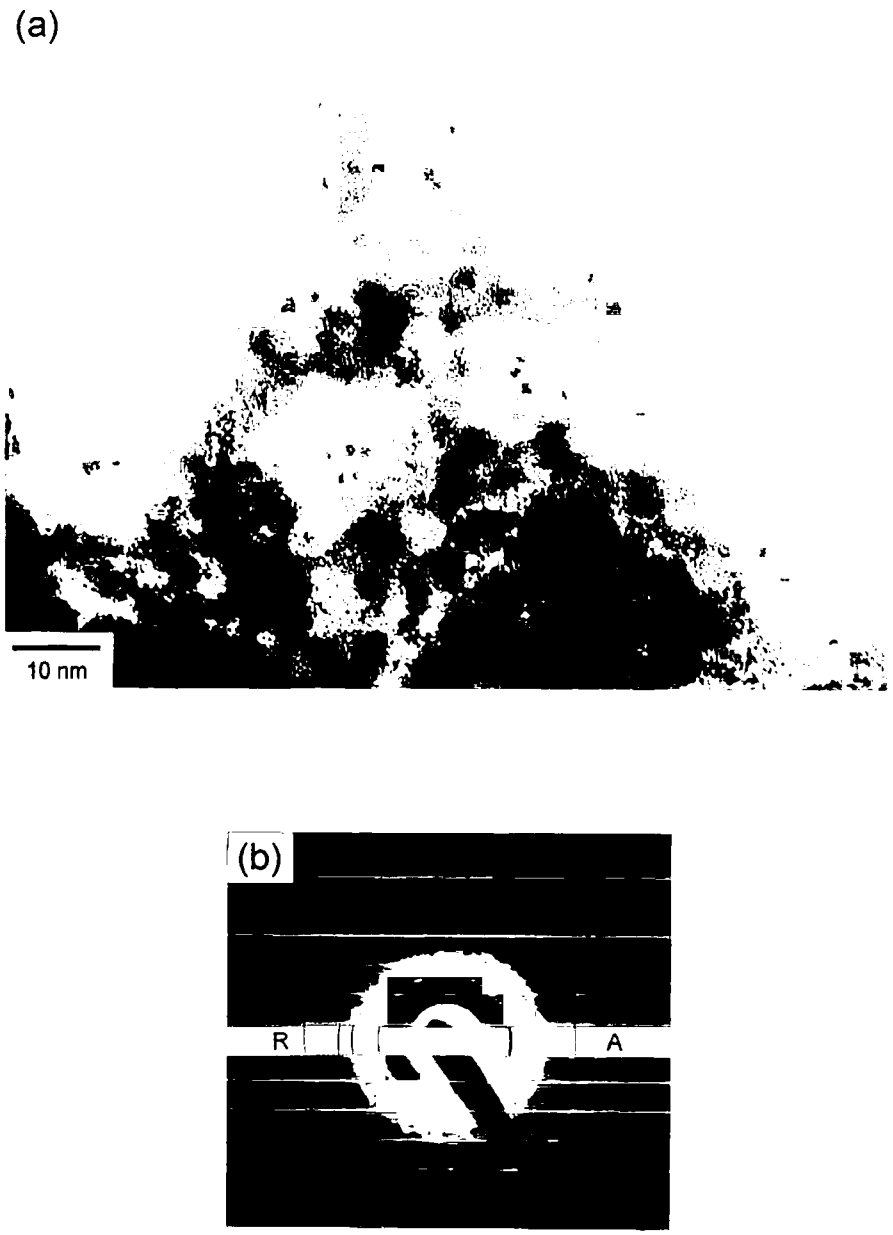

Fig. 2. 5. Transmission electron micrograph of the TO-2 (a) and its electron diffraction patterns (b) A and R correspond to the patterns of anatase and rutile, respectively.

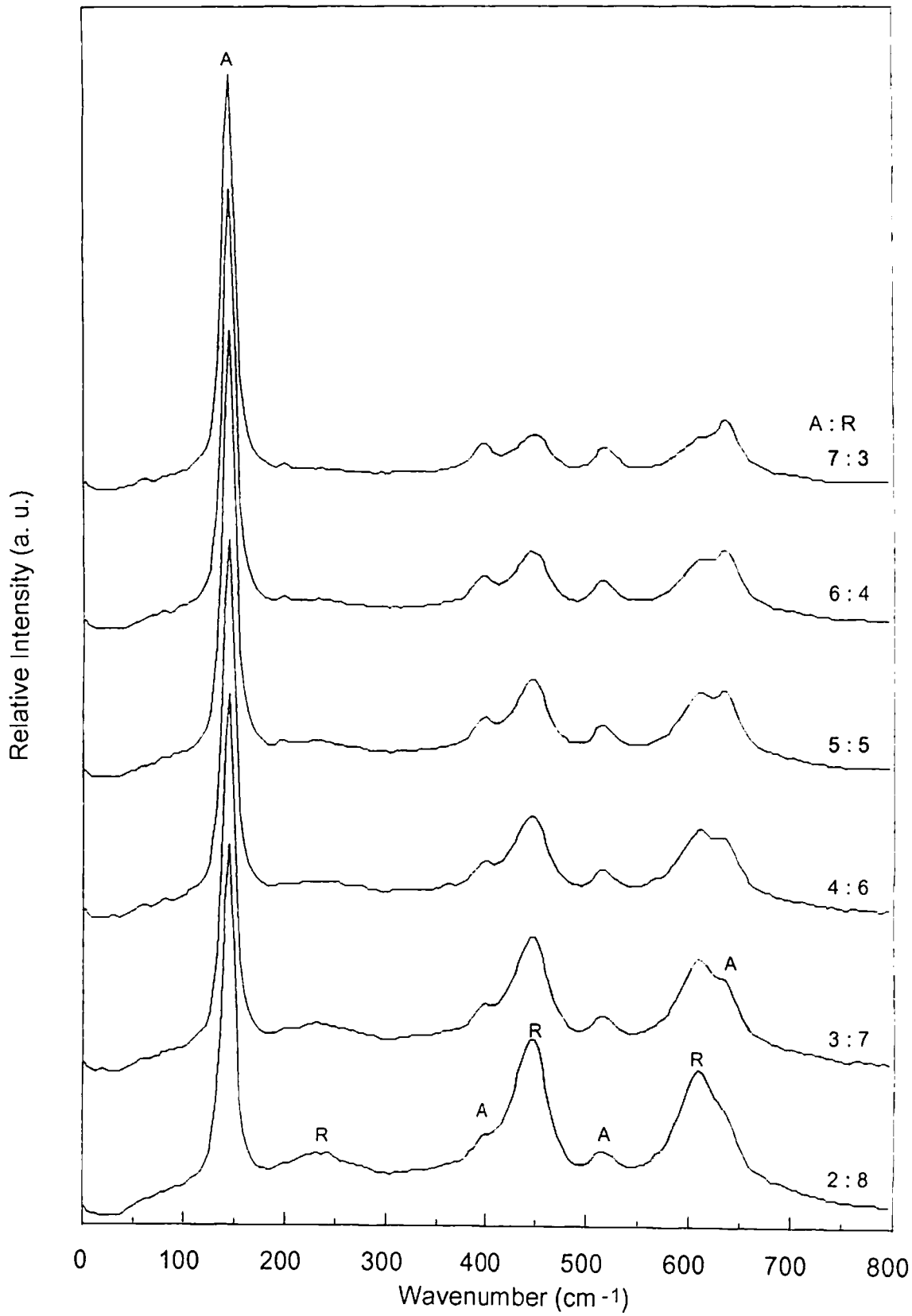

Fig. 2. 6. Raman spectra of mixed anatase-rutile phases. A and R peaks correspond to anatase and rutile phases.

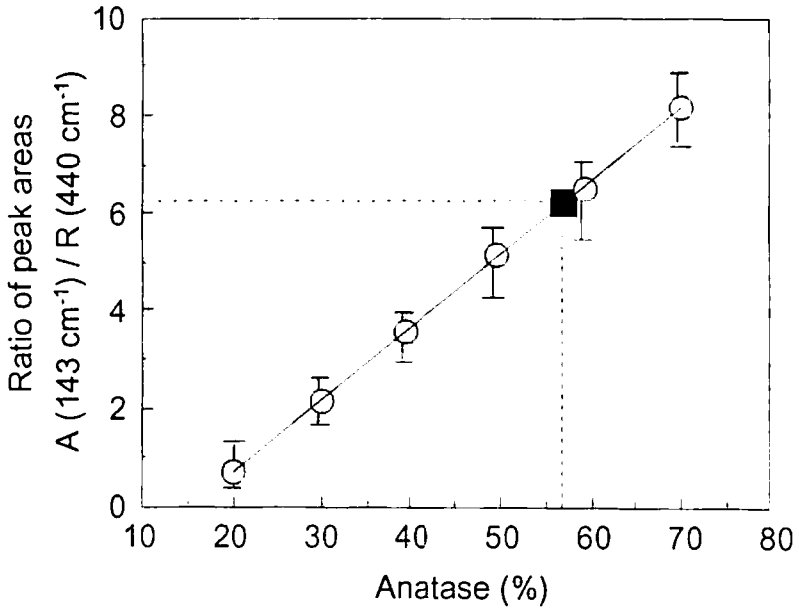

Fig. 2. 7. The ratio of the Raman peak area of anatase phase at 143 cm^{-1} to peak area of rutile phase at 440 cm^{-1} as a function of mixture percentage of anatase phase: (■) TO-2.

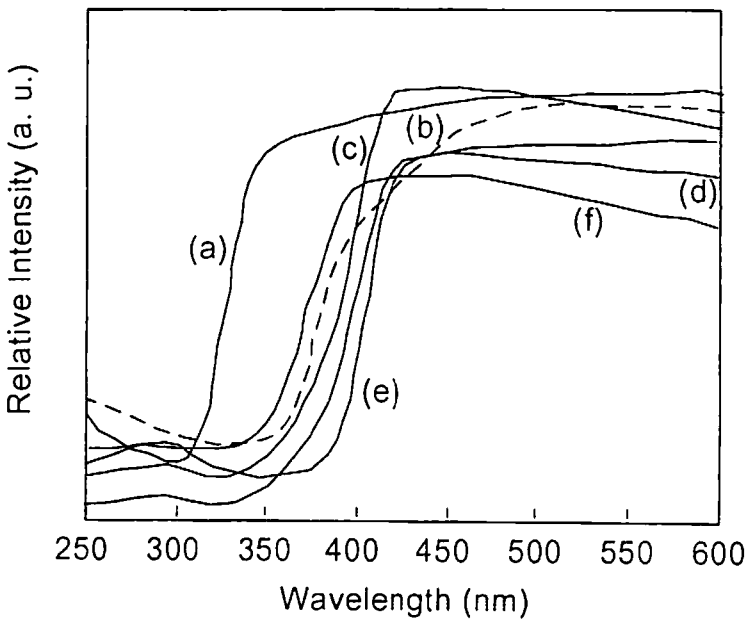

Fig. 2. 8. Absorption spectra of some TiO_2 samples: (a) TO-1, (b) TO-2, (c) P-25, (d) anatase, (e) rutile, and (f) amorphous.

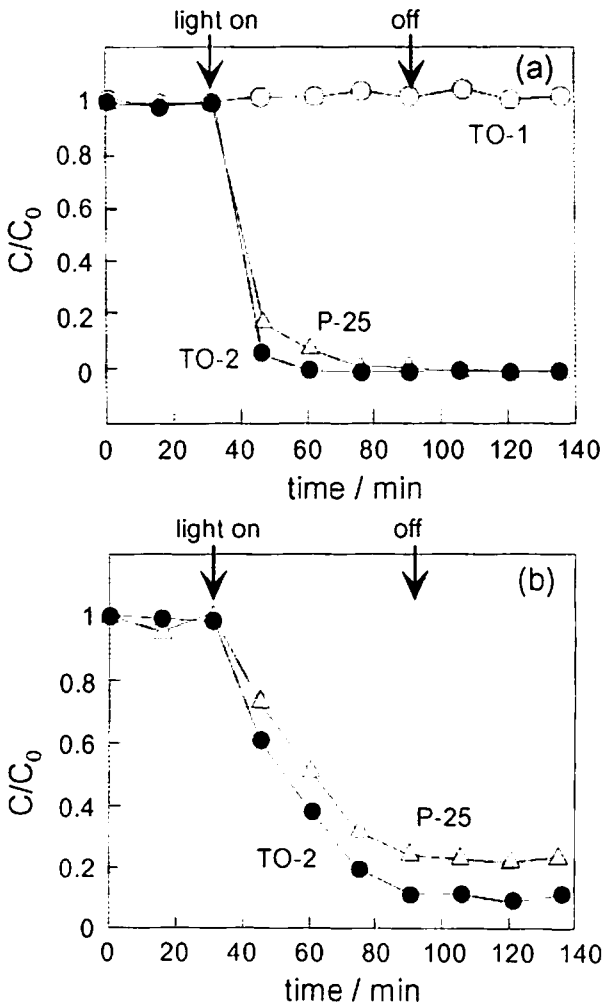

Fig. 2. 9. C (concentration)/ C_0 (initial concentration, ca. 10 ppm) as a function of the illumination time, irradiated by the xenon lamp (a) and by the F-lamp (b).

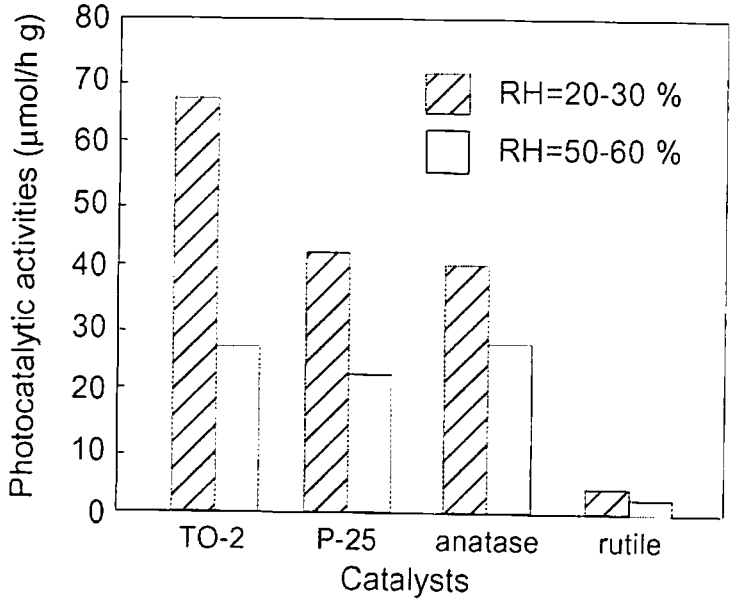

Fig. 2. 10. Specific photocatalytic activity per unit weight of the TiO_2 catalysts. The amount of the decomposed acetaldehyde per unit weight of various TiO_2 catalysts after 1 h of illumination with the 24 W fluorescent lamp was used as an indicator for the specific photocatalytic activity.

Chapter 3

Electrodeposition of TiO_2 Photocatalyst into Nano-Pores of Hard Alumite

3. 1 Introduction

We have developed a new low-cost electrochemical method for directly depositing TiO_2 photocatalyst onto an Al/Al_2O_3 substrate as stated in chapter 2.[1] However, the adhesion strength between TiO_2 and the alumite films was insufficient for practical use in this case, because two-step electrolysis for TiO_2 electrodeposition brings about an exfoliation of the film from the alumite surface. Consequently, tight adhesion between the TiO_2 and the alumite is necessary with the electrochemical method. In this study, one-step electrolysis for TiO_2 deposition was tested in order to improve the adhesion between the prepared Al_2O_3/TiO_2. This study discusses its photocatalytic activity as well as the deposition mechanism. Moreover, to improve the corrosion resistance, a hard alumite having a thicker barrier layer was used as the substrate alumite.

3. 2 Experimental

An aluminum plate (60 x 50 mm x 1 mm thick) was etched by immersion in alkaline solution and then electrochemically oxidized under 20 mA/cm^2 in H_2SO_4 solution (2.5 M) for 45 min at 2 °C to prepare the porous hard alumite on its surface (Al/Al_2O_3). TiO_2 was electrodeposited by alternative electrolysis into pores of alumite ($Al/Al_2O_3/TiO_2$) prepared by the previous method. The electrolysis was carried out in a mixed aqueous solution consisting of 10^{-2} M $(NH_4)_2[TiO(C_2O_4)_2]$ and 2.5 x 10^{-3} M $(COOH)_2$ adjusted to pH 4 by titration with NH_4OH, under an ac bias at 20 °C. The graphite plate (50 x 60 mm x 10 mm thick) was used as the counter electrode, and the distance between the counter and working electrodes was fixed at 50 mm. When the

electrolysis was carried out under ac bias, the current and voltage waveforms and the lissajous figure were observed with a synchroscope. An electrical resistance was introduced in the electric circuit in order to measure the electrolyzed currents and voltages as shown in Fig. 3. 1.

The morphology and elemental distribution of the prepared $Al/Al_2O_3/TiO_2$ were observed using electron probe microanalysis (EPMA). The amount of deposited TiO_2 was analyzed by inductively coupled plasma (ICP) spectroscopy, where the sample was dissolved in 1.2 M H_2SO_4 and then the solution was analyzed. The UV and visible absorption spectrum of the $Al/Al_2O_3/TiO_2$ and anatase (99.9 %, Wako, Ltd.) and rutile TiO_2 (99.9 %, Wako, Ltd.) were measured with a UV/VIS spectrophotometer.

The photocatalytic activity of the prepared $Al/Al_2O_3/TiO_2$ was measured for photodecomposition of acetaldehyde. A small amount of acetaldehyde gas was injected into a 1000 ml cylindrical quartz cell (62.5 cm^2 x 16 cm; concentration about 30 ppm), where the $Al/Al_2O_3/TiO_2$ was fixed in the cell in advance, and then illuminated. A 500 W xenon lamp (200 mW/cm^2) was used as the light source.

3. 3 Results and Discussion

3. 3.1 Electrodeposition of TiO_2

Figure 3. 2 shows the amount of TiO_2 deposited in the pores of the alumite after 10 minutes as a function of the applied maximum ac voltage. Most of the voltage was applied to the alumite because of the very low resistance of the electrolyte (14.57 mS/cm). The amount of TiO_2 in the $Al/Al_2O_3/TiO_2$ was about 0.5 x 10^{-5} g/cm^2 in the ac voltage region of less than about 8 V. However, this amount increased with the increase in the ac voltage region of over that about 9 V. When the applied voltage exceeded about 13 V, the alumite was exfoliated from the aluminum substrate within 10 minutes. Figure 3. 3 shows the amount of deposited TiO_2 as a function of electrolysis time. For

an applied maximum voltage of 11 V, the amount of TiO_2 slightly increased with an increase in electrolysis time. However, for an applied maximum voltage of 12 V, removal of the alumite film occurred after 12 minutes and then the solution became violet together with H_2 evolution on the Al substrate surface.[2] In this case, TiO_2 deposition occurred directly on aluminum metal surface. Consequently, the total amount of the deposited TiO_2 increased with electrolysis time of less than 15 minutes, but decreased at 20 min because of the removal of the deposited TiO_2 as shown in Fig. 3. 3. Thus, 10 min was the most suitable electrolysis time for the present preparation of the $Al/Al_2O_3/TiO_2$ under ac 12 V.

Figure 3. 4 shows the lissajous figures of current versus applied voltage in $(NH_4)_2[TiO(C_2O_4)_2]$ aqueous solution. The dashed and solid ellipses correspond to the applied maximum ac voltages of 8 and 12 V, respectively. For the 8 V applied bias, the ellipse was inclined slightly. The incline is due to the phase difference between the current and the voltage waveform, since the barrier layer in the alumite has the ability to store charges like a capacitor.[2,3] However, for the electrolysis at 12 V, the distorted ellipse was observed at around –10 V. The cathodic current increased rapidly in the voltage region more negative than about –10 V. Lissajous similar to that shown in Fig. 3. 4 (a) was also observed for Na_2SO_4 solution adjusted to pH 4 by titration with NH_4OH solution as shown in Fig. 3. 4 (b). The ellipse's distortion indicates a corresponding distortion of the sine wave due to a reaction current.[2] In both $(NH_4)_2[TiO(C_2O_4)_2]$ and Na_2SO_4 solutions, hydrogen generation on the surface of the alumite was observed during 12 V electrolysis, but not at 8 V bias. Thus, the cathodic current at about –10 V was due to the hydrogen evolution. In conclusion, TiO_2 is deposited under a cathodic process in the ac electrolysis with an applied bias of more than about 10 V (Fig. 3. 2). The electrodeposition of TiO_2 by the cathodic process during the ac electrolysis probably proceeds in the pores of alumite as follows:

$(NH_4)_2[TiO(C_2O_4)_2] \rightarrow TiO(C_2O_4)_2^{2-} + 2NH_4^+$ (1)

$2H_2O + 2e^- \rightarrow H_2$ (and/or $2H_{ads}$) $+ 2OH^-$ (2)

$TiO(C_2O_4)_2^{2-} + 2OH^- \rightarrow TiO_2 + H_2O + 2(C_2O_4)^{2-}$ (3)

$(NH_4)_2[TiO(C_2O_4)_2]$ will dissolve to dissociate into $TiO(C_2O_4)_2^{2-}$ and ammonium ions (eq 1) in aqueous solution in advance of the electrolysis. Cathodic bias during the ac electrolysis will bring about an electrochemical reaction (2) where OH^- ion is produced. Finally, TiO_2 was produced in the pores of the alumite films by the reaction (3). In fact, TiO_2 was precipitated in a beaker, when the pH of the solution containing $(NH_4)_2[TiO(C_2O_4)_2]$ was adjusted from 4 to about 5 by titration of the NH_4OH solution.

3. 3. 2 Characterization of deposited TiO_2

The absorption spectra of the present TiO_2 deposited on alumite and other TiO_2 samples (anatase and rutile powder: 0.3 μm average particle size) are shown in Figure 3. 5. The deposited TiO_2 ((a)-(f)) showed absorption in the wavelength region shorter than about 330 nm. Thus, relatively blue shifts were observed for the deposited TiO_2 ((a)-(d)) unlike the anatase (e) and rutile (f) powders. A similar blue shift has been already observed for the quantized TiO_2 particles and/or highly dispersed TiO_2 in the porous substrate.[4-8] The blue shift in the deposited TiO_2 is probably due to the highly dispersed state of the nano-sized TiO_2 in the pores of alumite, because the TiO_2 was roughly estimated to be deposited from a monolayer to 10 layers, as discussed later. The absorption spectrum of the $Al/Al_2O_3/TiO_2$ heated to 500 °C slightly shifted to a longer wavelength. This suggests that the deposited TiO_2 particles were scarcely aggregated by the heat-treatment to produce large size particles because of the high dispersion.

Figure 3. 6 (a) shows the line profile of the EPMA elemental distribution in the cross section of the $Al/Al_2O_3/TiO_2$ prepared at 12 V ac bias for 10 min. The part where Al overlaps with O in the distribution corresponds to the alumite film formed on the Al

substrate. The thickness of the present alumite layer was estimated to be about 25-30 μm. From Figure 3. 6 (a), it was estimated that about 35 % of the deposited TiO_2 exists in the pore region from the bottom to 5 μm thickness. The total amount of deposited TiO_2 in one pore in the alumite was estimated from the amount of TiO_2 analyzed by ICP measurement to be 4.2×10^{-16} g, where the number of pores of the present alumite is assumed to be 77×10^9 /cm^2.[2] That is, about 1.5×10^{-16} g of TiO_2 exists in the above bottom region in one pore. If deposited TiO_2 exists with 100 % density as anatase or rutile phase in the pore walls (radius: 10 nm[9]) from the bottom to 5 μm thickness, the average thickness of the TiO_2 in this pore region is estimated to be less than 2 nm (a few TiO_2 layers). The amount of deposited TiO_2 was highest at the bottom of the pores and decreased with distance to the top. Consequently, it was suggested that TiO_2 exists with mono-10 layers on the walls of the pores as shown in Figure 3. 6 (b).

The adhesion strength between the deposited TiO_2 and the alumite was insufficient in the case of two-step electrolysis as stated in the chapter 2.[1] This is based on the presence of the deposited TiO_2 mainly on the surface of alumite. On the other hand, the TiO_2 deposited by the present one-step electrolysis existed in the pore of alumite as described above, leading to strong adhesion. In practice, most of the TiO_2 deposited by the two-step electrolysis was removed from the alumite, but not for that deposited by the one-step electrolysis, according to a Scotchtape adhesion peel test. Consequently, an improvement of the adhesion between the deposited TiO_2 and the alumite was accomplished by the present one-step electrolysis.

No diffraction peak in XRD measurement was observed even for the heat-treated TiO_2 at 500 °C, because the amount of deposited TiO_2 in the pores of alumite is too small to be detected. Moreover, no Raman peak due to anatase and rutile phase was observed for the deposited TiO_2. This may be due to the dispersed state of the deposited TiO_2 as well as its small amount, since the field strength of isolated TiO_2 particles is

much weaker than that of the aggregated particles.[10]

3. 3. 3 Photocatalytic activity of the $Al/Al_2O_3/TiO_2$.

Figure 3. 7 shows the concentration of acetaldehyde as a function of illumination time, when the $Al/Al_2O_3/TiO_2$ samples were prepared at 10 and 12 V for 10 min. The concentration gradually decreased with illumination for both samples, indicating that the deposited TiO_2 into alumite pores has photocatalytic activity. The apparent photocatalytic activity is higher for the samples prepared at 12 V than that at 10 V, indicating that the amount of the TiO_2 is important in this case, as shown in Fig. 3. 2.

Figure 3. 8 shows the relationship between the photocatalytic activity and the amount of deposited TiO_2 for the $Al/Al_2O_3/TiO_2$ prepared at 11 V and 12 V for 12 min. The photocatalytic activity was evaluated from the ratio of the amount of acetaldehyde decomposed during 1 h illumination to that of the initial acetaldehyde. The activity of the TiO_2 deposited at 12 V was lower than that of the TiO_2 deposited at 11 V, although the amount of the TiO_2 is greater for the former sample than for the latter sample. This will be based on the difference in the substrate. The high photocatalytic activity of TiO_2 anchored in pore walls of the alumite will be due to two factors: (i) TiO_2 in the pores of alumite was quantized (many reports have shown that quantized semiconductor photocatalyst has a high photocatalytic activity because of the increase in bandgap energy[6,11,12] and the decrease of the distance which the photoinduced holes and electrons have to diffuse before reaching the interface[13]) (ii) highly dispersed TiO_2 has a large surface area compared to that of TiO_2 particles on aluminum substrate. More study is needed to explain which effect contributes to the high photocatalytic activity.

3. 4 Conclusions

In conclusion, electrodeposition of TiO_2 photocatalyst into the pores of the hard alumite (thick Al_2O_3 film) was followed by use of an ac electrolysis technique. TiO_2 was deposited by increase in the pH in the pores in the cathodic process during the ac electrolysis. TiO_2 was dispersed in several layers on the pore walls, and showed high photocatalytic activity. It is suggested that the dispersed state of the deposited TiO_2 is important for high catalytic activity. The prepared $Al/Al_2O_3/TiO_2$ plate will be practically useful because the hard alumite is a corrosion-resistant.

References

(1) Matsumoto, Y.; Ishikawa, Y.; Nishida, M.; Ii, S. *J. Phys. Chem. B* **2000,** 104, 4204.

(2) Mita, I.; Kuroda, K.; Suzuki, K.; Muramatsu, Y.; Nemoto, S.; Yamada, M. *Handbook of Aluminium Surface Treatment;* Light Metal Publishing: Tokyo, 1980.

(3) Sato, T.; Sakai, S. *Trans. Inst. Met. Finish.* **1979,** 57, 43.

(4) Anpo, M.; Aikawa, N.; Kubokawa, Y.; Che, M.; Louis, C.; Giamello, E. *J. Phys. Chem.* **1985,** 89, 5017.

(5) Liu, X.; Lu, K. K.; Thomas, J. K. *J. Chem. Soc., Faraday Trans.* **1993,** 89. 1861.

(6) Uchida, H.; Hirao, S.; Torimoto, T.; Kuwabata, S.; Sakata, T.; Mori, H.; Yoneyama. H. *Lngmuir* **1995,** 11, 3725.

(7) Domen, K.; Sakata, Y.; Kudo, A.; Maruya, K.; Onishi, T. *Bul. Chem. Soc. Jpn.* **1988,** 61, 359.

(8) Yamashita, H.; Ichihashi, Y.; Anpo, M.; Hashimoto, M.; Louis, C.; Che, M. *J. Phys. Chem.* **1996,** 100, 16041.

(9) González, J. A.; López, V.; Bautista, A.; Otero, E. *J. Appl. Electrochem.* **1999,** 29 229.

(10) Suh, J. S.; Lee, J. S. *Chem. Phys. Lett.* **1997,** 281, 384.

(11) Shiragami, T.; Pac, C.; Yanagida, S. *J. Phys. Chem.* **1990,** 94, 504.

(12) Anpo, M.; Shima, T.; Kodama, S.; Kubokawa, Y. *J. Phys. Chem.* **1987,** 91, 4305.

(13) Wu, J.; Uchida, S.; Fujishiro, Y.; Yin, S.; Sato, T. *J. Photochem. Photobiol.. A* **1999,** 128, 129.

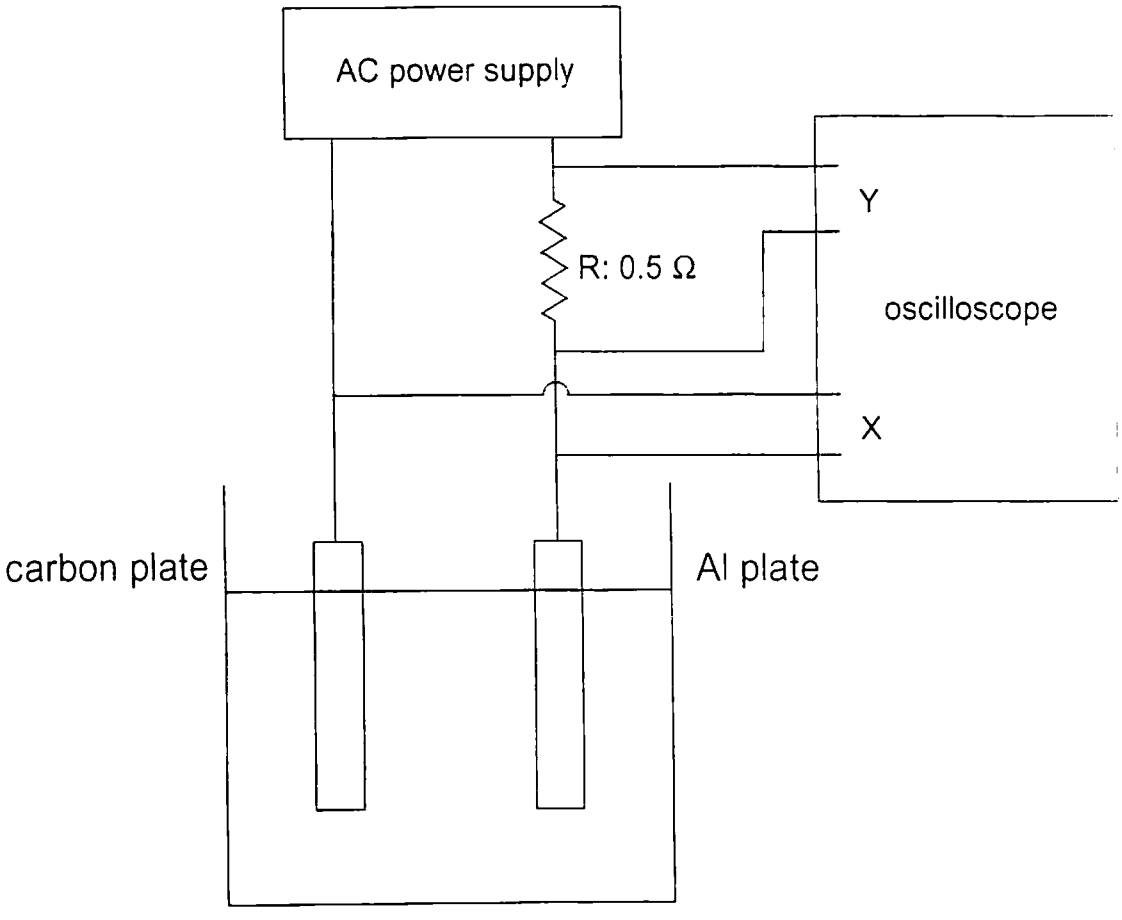

Fig. 3. 1. Measurement system of Lissajous figure.

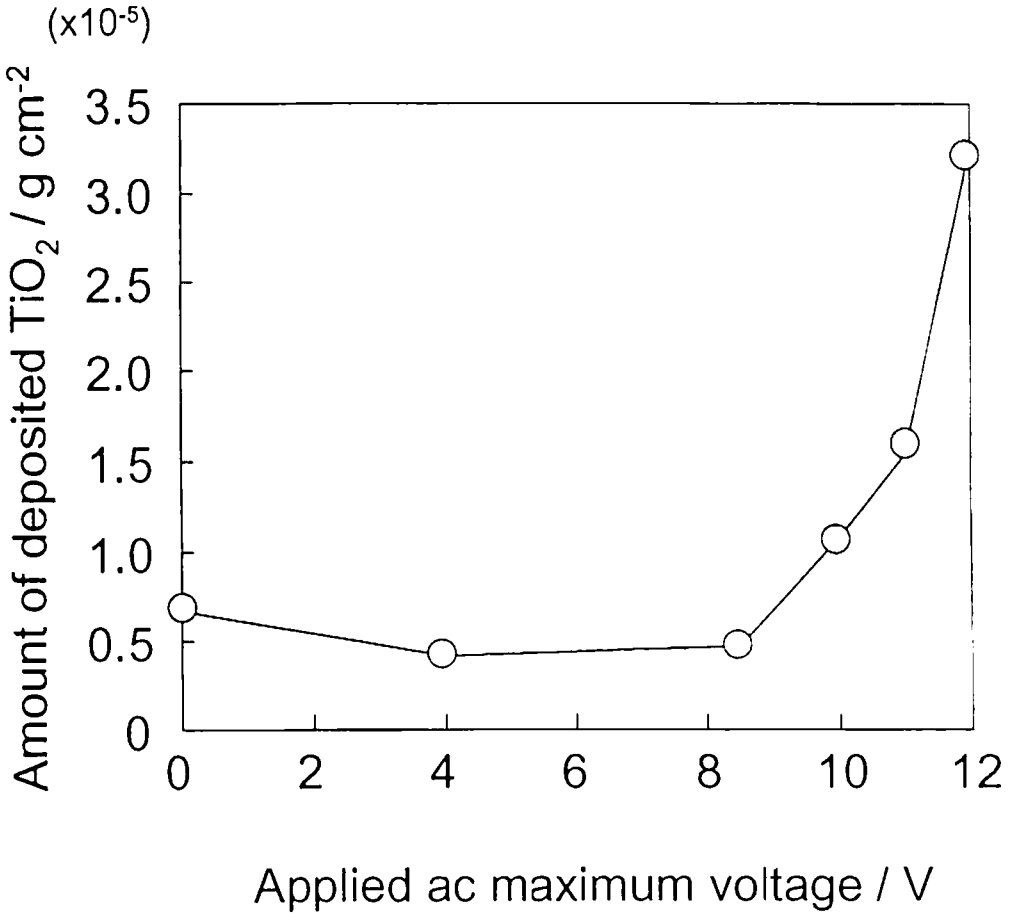

Fig. 3. 2. Amount of deposited TiO_2 as a function of applied maximum ac voltage. The electrolysis time was 10 min.

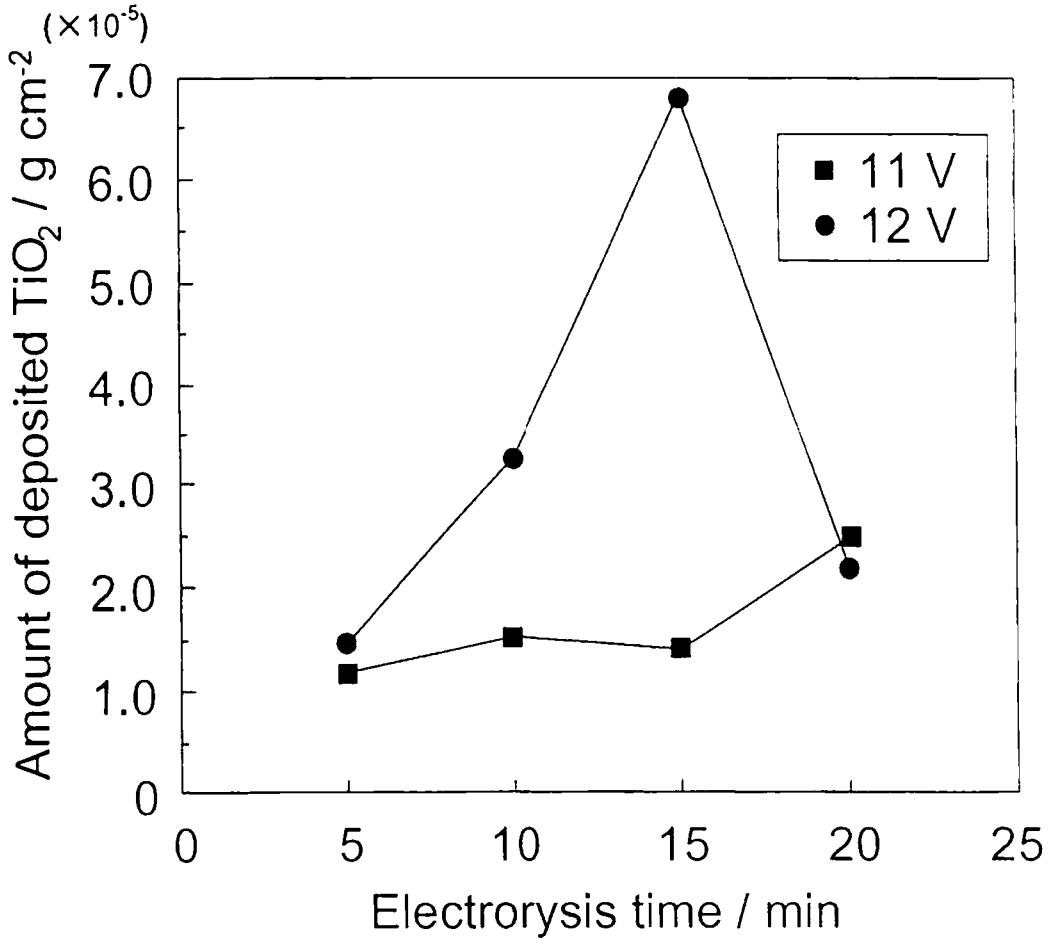

Fig. 3. 3. Amount of deposited TiO_2 as a function of electrolysis time. The maximum as voltages were 11 and 12 V.

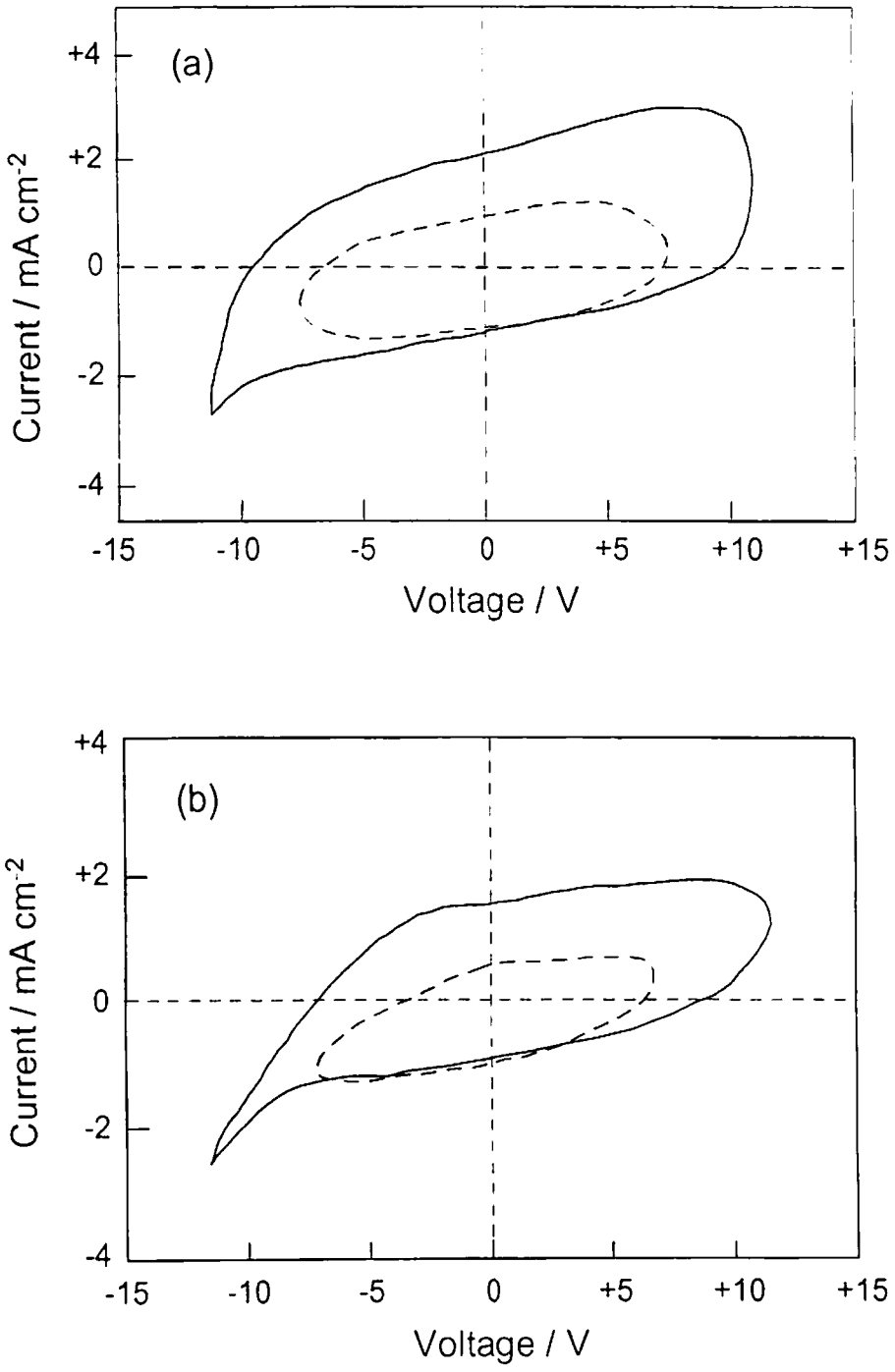

Fig. 3. 4. Lissajous figures of alumite in aqueous solution of $(NH_4)_2[TiO(C_2O_4)_2]$ (a) and Na_2SO_4 (b). The dashed and solid ellipses correspond to applied ac maximum voltages of 8 and 12 V, respectively.

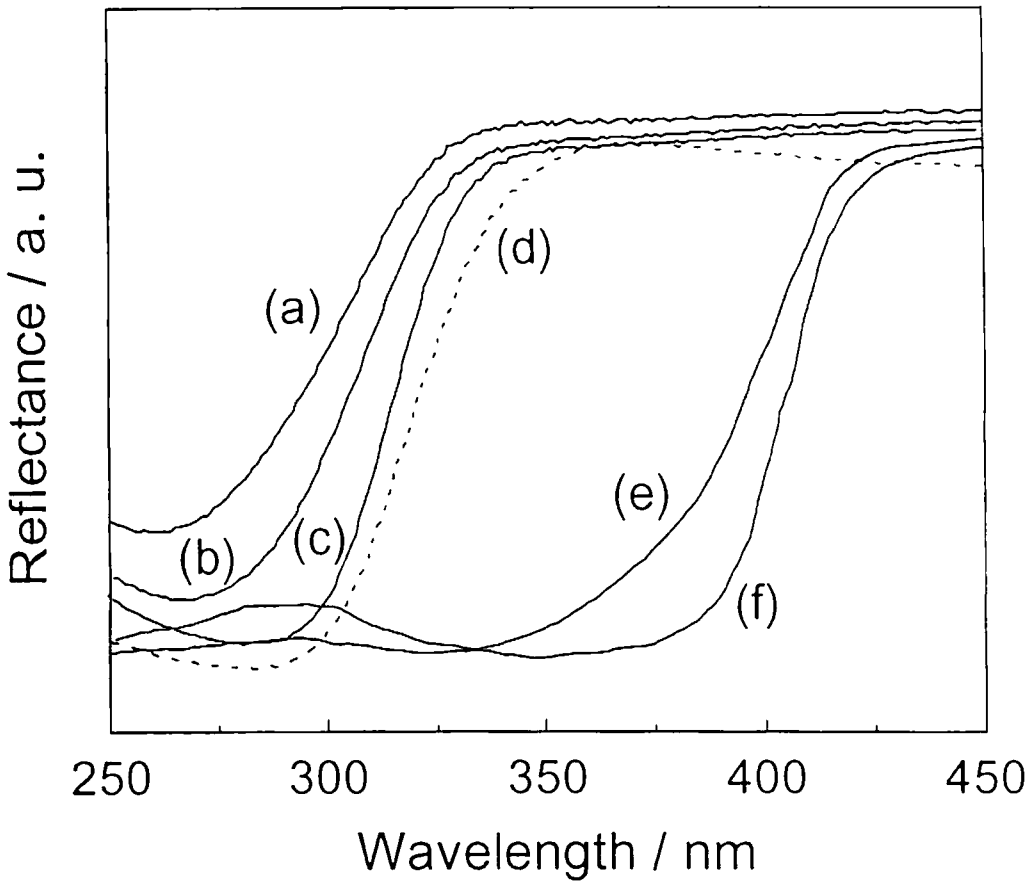

Fig. 3. 5. Absorption spectra of Al/Hard-Al_2O_3/TiO_2 prepared at various ac voltages: (a) 10; (b) 11; (c) 12 V; (d) heat-treated (d) sample; (e) anatase powder (0.3 μm); and (f) rutile powder (0.3 μm).

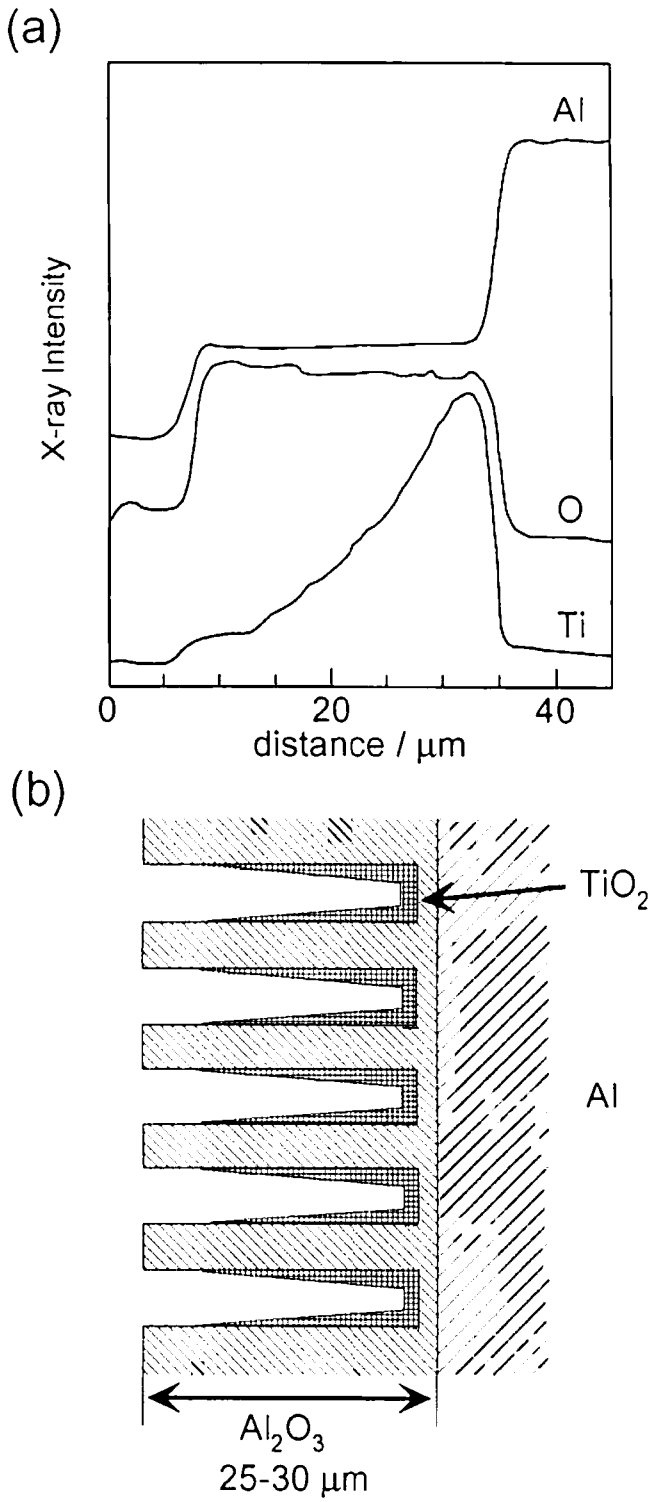

Fig. 3. 6. Line profile of EPMA elemental distribution in cross-section of the $Al/Al_2O_3/TiO_2$ at ac 12 V (a) and its model (b).

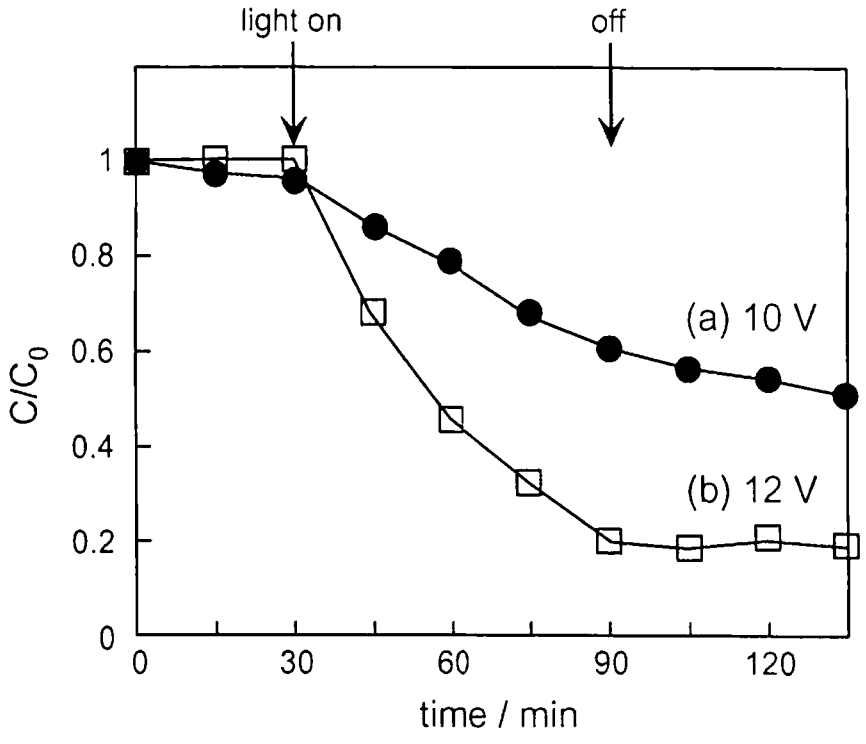

Fig. 3. 7. C (concentration)/C_0 (initial concentration, ca. 30 ppm) as a function of illumination time. Al/Al_2O_3/TiO_2 were prepared at 10 V for 10 min (a) and at 12 V for 10 min (b).

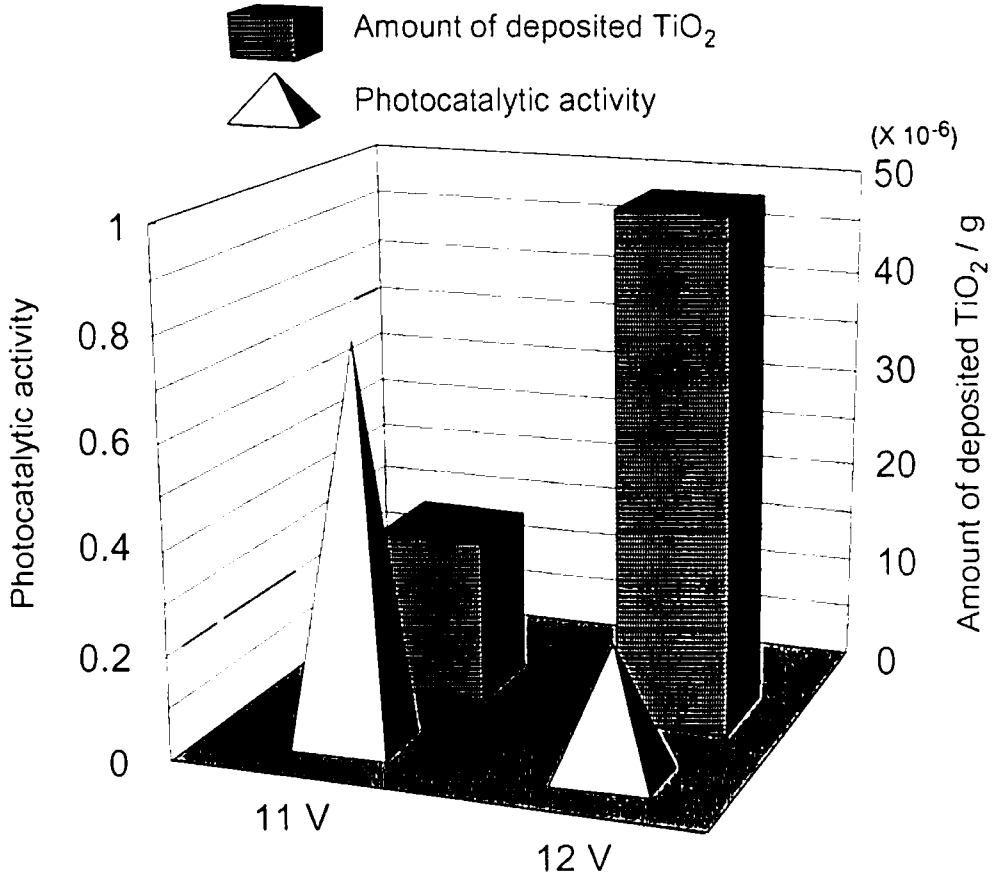

Fig. 3. 8. Relationships between the amount of deposited TiO_2 and photocatalytic activity for applied maximum ac voltage of electrolysis for 12 min.

Chapter 4

Preparation of TiO_2 Film Fixed on Hard Alumite Substrate

4. 1 Introduction

We have developed new low-cost electrochemical methods for directly depositing the TiO_2 photocatalyst onto an Al/Al_2O_3 substrate (denoted by $Al/Al_2O_3/TiO_2$). In these cases, the electrodeposition has been made by the two-step (chapter 2) or one-step (chapter 3) electrolysis.[1,2] In the former case, the as-deposited TiO_2 consisted of mixtures of the anatase, rutile, and amorphous phases, and showed high photocatalytic activity. However, the adhesion strength between the TiO_2 and the Al/Al_2O_3 substrate was insufficient for practical use. On the other hand, in the latter case, although the deposited TiO_2 showed low photocatalytic activity compared with that deposited by the two-step electrolysis because of its relatively small amount, an improvement in the adhesion between the deposited TiO_2 and the Al/Al_2O_3 substrate was accomplished. In this study, it is demonstrated that the Al/Al_2O_3 (hard alumite)/TiO_2 prepared by the one-step electrolysis showed high photocatalytic activity due to the increase in its amount by the temperature control of the electrolyte. Moreover, the most optimal preparation conditions were determined for the $Al/Al_2O_3/TiO_2$ from a comparison of the photocatalytic activity and adhesion strength between the TiO_2 and the Al/Al_2O_3 substrate.

4. 2 Experimental

An aluminum plate (60 x 50 x 1 mm thick) was etched by immersion in alkaline solution and then electrochemically oxidized at 20 mA cm^{-2} in H_2SO_4 solution (2.5 M) for 45 min at 2 °C to prepare the porous hard alumite on its surface (Al/Al_2O_3). TiO_2 was electrodeposited by alternative electrolysis (60 Hz) or precipitated into the

pores of the alumina film prepared by the previous method ($Al/Al_2O_3/TiO_2$). The TiO_2 deposition was carried out in a mixed aqueous solution consisting of 10^{-2} M $(NH_4)_2[TiO(C_2O_4)_2]$ and 2.5 x 10^{-3} M $(COOH)_2$ adjusted to pH 4 by titration with NH_4OH, for 10 min at various temperatures. A graphite plate (50 x 60 x 10 mm thick) was used as the counter electrode, and the distance between the counter and working electrode was fixed at 50 mm.

The morphology and elemental distribution of the prepared $Al/Al_2O_3/TiO_2$ were observed using electron probe microanalysis (EPMA). The amount of the deposited TiO_2 was analyzed by inductively coupled plasma (ICP) spectroscopy, where the sample was dissolved in 1.2 M H_2SO_4 and then the solution was analyzed. The UV and visible absorption spectrum of the $Al/Al_2O_3/TiO_2$, anatase (99.9 %, Wako, Ltd.) and rutile TiO_2 (99.9 % Wako, Ltd.) were measured with a UV-Vis spectrophotometer. The structure of the TiO_2 films after the heat treatment was examined by X-ray diffraction analysis (XRD) using monochromatic CuKα radiation.

The photocatalytic activity of the prepared $Al/Al_2O_3/TiO_2$ was measured for the photodecomposition of acetaldehyde. A small amount of acetaldehyde gas was injected into a 1000 ml cylindrical quartz cell (62.5 cm^2 x 16 cm), where the $Al/Al_2O_3/TiO_2$ had been previously fixed in the cell, and then illuminated. A 500 W xenon lamp (200 mW cm^{-2}) and a 24 W fluorescent lamp (rare-earth lamp, Mitsubishi-BS3601B, 10 mW cm^{-2}) were used as the light sources.

4. 3 Results and discussion

4. 3. 1 Deposition of TiO_2

Figure 4. 1 shows the amount of TiO_2 deposited on the Al/Al_2O_3 substrate under various temperatures as a function of the applied maximum ac voltage. Most of the voltage was applied to the alumite side because the resistance of the electrolyte is very

low (14.57 mS cm^{-1}). The amount of TiO_2 in the $Al/Al_2O_3/TiO_2$ was about 0.5 x 10^{-5} g cm^{-2} in the voltage region less than about 8 V at 20 °C. However, this amount increased with the increase in the voltage region higher than about 9 V. In the electrodeposition process of the TiO_2, the cathodic bias during the ac electrolysis above 9 V brings about the reduction of H^+ and/or H_2O, leading to deposition of TiO_2 due to the pH increase in the pores of the alumina film.

It should be noted that the amount of deposited TiO_2 remarkably increased with the increase in the electrolyte temperature. The amount of deposited TiO_2 did not depend on the ac voltage, and the deposition occurred even under no bias. Figure 2 shows an Arrhenius plot of the amount of the deposited TiO_2 as a function of temperature. For the non-applied voltage (b), the log(amount of deposited TiO_2) increased linearly with K^{-1}, but not for the applied ac 12 V (a), where two regions are observed in the temperature dependence. The amount of the deposited TiO_2 depends on the applied ac voltage at 20 °C as shown in Figs. 4. 1 and 2, when the voltage is higher than about 9 V. Consequently, the electrodepositionon of TiO_2 predominantly occurs in the region of less than about 50 °C, while chemical deposition predominantly occurs at temperatures higher than about 50 °C. The activation energy of the chemical deposition was estimated to about 48.6 $kJmol^{-1}$ from the slope in Fig. 4. 2. Under a non-applied ac voltage, the TiO_2 chemical deposition mainly occurred on the Al/Al_2O_3 substrate according to the Fig. 4. 2 analysis, since $TiO(C_2O_4)_2^{2-}$ existing in the $(NH_4)_2[TiO(C_2O_4)_2]$ solution at pH 4 will strongly adsorb on alumina surface whose pH value at point of zero charge (PZC) is about 8.[3,4] The chemical deposition of the TiO_2 under a non-applied ac voltage will occur on the surface of alumina as follows:

$$(NH_4)_2[TiO(C_2O_4)_2] \rightarrow TiO(C_2O_4)_2^{2-} + 2NH_4^+ \qquad (1)$$

$$2AlOH_2^+{}_{surf} + TiO(C_2O_4)_2^{2-} + H_2O \rightarrow Al_2O_2TiO(H_2O)_{surf} + 2(C_2O_4)^{2-} + 4H^+ \qquad (2)$$

$(NH_4)_2[TiO(C_2O_4)_2]$ will dissolve and then dissociate into $TiO(C_2O_4)_2^{2-}$ and ammonium

ions (eq. 1) in aqueous solution. The protonated surface of alumina at pH 4 will adsorb the $TiO(C_2O_4)_2^{2-}$, leading to the formation of Al-O-Ti and the deposition of TiO_2 which will be hydrated (eq. 2).

4. 3. 2 UV absorption spectra of the deposited TiO_2

Some absorption spectra of the present TiO_2 deposited on the Al/Al_2O_3 substrate and other TiO_2 samples (anatase and rutile powders: 0.3 μm average particle size) are shown in Figure 4. 3. The deposited TiO_2 at 20 (a) and 50 °C (b) showed absorption in the wavelength region shorter than about 350 nm. Thus, the deposited TiO_2 at 20 and 50 °C showed a blue shift compared with the anatase (d) and rutile (e) samples. The blue shift in these TiO_2 will be due to the quantized TiO_2 particle and/or highly dispersed state of the nano-sized TiO_2 in the pores of the alumina film[5-7], because the TiO_2 was roughly estimated to be deposited from a monolayer to ten layers, as discussed in chapter 3.[2] On the other hand, the deposited TiO_2 at 90 °C was similar to the anatase powder (d). This suggests that the deposited TiO_2 at 90 °C were bulk particles.

4. 3. 3 Photocatalytic activity of the $Al/Al_2O_3/TiO_2$

Figure 4. 4 shows the concentration of acetaldehyde (C) as a function of the illumination time. In Figure 4. 4(a), a 500 W xenon lamp was used as the light source for the $Al/Al_2O_3/TiO_2$ prepared at 12 V at various temperatures, where the initial concentration (C_0) of acetaldehyde was 30 ppm. The concentration gradually decreased with illumination for all the samples, indicating that the deposited TiO_2 on Al/Al_2O_3 substrate has photocatalytic activity. The apparent photocatalytic activity increased with an increase in the temperature of the electrolyte, because the amount of the deposited TiO_2 increased with the temperature of the electrolyte. The catalytic activity of the TiO_2 hardly depended on the applied voltage when the electrolysis was done at temperatures

higher than about 50 °C. Consequently, the photocatalytic activity of the prepared $Al/Al_2O_3/TiO_2$ mainly depends only on the amount of the deposited TiO_2.

In Figure 4. 4(b), a 24 W fluorescent lamp (F-lamp) was used as the light source for the $Al/Al_2O_3/TiO_2$ prepared at 90 °C, where the initial concentration of acetaldehyde was 10 ppm. The $Al/Al_2O_3/TiO_2$ (as-deposited at 90 °C) showed only a slight activity, while the $Al/Al_2O_3/TiO_2$ heat-treated at 550 °C for 1 h showed high activity even under fluorescent lamp illumination. Figure 4. 5 shows the XRD patterns of the $Al/Al_2O_3/TiO_2$ prepared at 12 V and 90 °C. From the XRD patterns of the $Al/Al_2O_3/TiO_2$ heat-treated at temperatures higher than 450 °C, only anatase is produced by the heat-treatment. Thus, the heat treatment temperature higher than 450 °C causes the crystallization to anatase, bringing about the high photocatalytic activity, as shown in Figure 4. 4(b). The activity of the $Al/Al_2O_3/TiO_2$ heat-treated at 450 °C for 1 h was similar to that at 550 °C.

4. 3. 4 Morphology of the $Al/Al_2O_3/TiO_2$

Figures 4. 6(a)-(c) and (d)-(f) show the line profile of the EPMA elemental distribution in the cross-section of the Al/Al_2O_3 with TiO_2 electrodeposited at 12 V under various temperatures and their models. The section where Al overlaps with O in the distribution corresponds to the alumina film formed on the Al. The thickness of the alumina film was estimated to be about 25-30 μm. Ti was mainly deposited in the bottom portion of the pores of the alumina film at 20 °C ((a) and (d)). On the other hand, the distribution of Ti was shifted to the surface of the alumina film with the temperature of the electrolyte as shown in (b), (c), (e), and (f). According to the X-ray photoelectron spectroscopy (XPS) measurement of the surface of the $Al/Al_2O_3/TiO_2$, TiO_2 on surface of the Al/Al_2O_3 substrate was detected for the deposition at 70 and 90 °C. but not at 50 °C. Probably, the hydration of alumina (denoted as $Al_2O_3 \cdot nH_2O$) might be formed at the

bottom of the pores of the alumina film by immersion in the high temperature aqueous solution. Therefore, the pores of the alumina film were sealed with the produced hydrated alumina at high temperatures, leading to the change in the deposited TiO_2 location as shown in Fig. 4. 6 (f). For the precipitation at 20 °C, Ti was not detected, because the amount of the deposited TiO_2 was quite low. The differences in the Ti distribution were not observed at 50 and 90 °C, respectively, whether the electrolysis was carried out or not.

In the chapter 3, an improvement in the adhesion between the deposited TiO_2 and the Al/Al_2O_3 substrate was accomplished by the presence of the deposited TiO_2 in the pores of the alumina film. Consequently, the TiO_2 deposition in the pore of the alumina film at temperatures less than about 70 °C is also preferable for the strong adhesion between the TiO_2 and the Al/Al_2O_3 substrate. In practice, most of the TiO_2 deposited at temperatures higher than 70 °C was removed from the Al/Al_2O_3 substrate, but not for that at 50 °C, based on a Scotchtape adhesion peel test.

4. 4 Conclusions

In conclusion, an improvement in the photocatalytic activity of the $Al/Al_2O_3/TiO_2$ was accomplished by increasing the temperature of the TiO_2 deposition. However, the adhesion strength between the deposited TiO_2 and the Al/Al_2O_3 substrate was insufficient for the TiO_2 deposition at 90 °C, because the deposited TiO_2 mainly existed on the surface of the Al/Al_2O_3 substrate. The $Al/Al_2O_3/TiO_2$ prepared at 50 °C, which showed a relatively high photocatalytic activity, was the most preferable for practical use, because most of the deposited TiO_2 existed in pores of the alumina film.

References

(1) Matsumoto, Y.; Ishikawa, Y.; Nishida, M.; Ii, S. *J. Phys. Chem. B* **2000,** 104, 4204.

(2) Ishikawa, Y.; Matsumoto, Y. *Electrochim. acta* **2001,** 46, 2819.

(3) Xiong, G.; Feng, Z.; Li, J.; Yang, Q.; Ying, P.; Xin, Q.; Li, C. *J. Phys. Chem. B* **2000,** 104, 3581.

(4) Alosio, M. A. C.; Jean, G. E. *Appl. Catal. A* **1998,** 167, 203.

(5) Liu, X.; Lu, K. K.; Thomas, J. K. *J. Chem. Soc., Faraday Trans.* **1993,** 89, 1861.

(6) Uchida, H.; Hirao, S.; Torimoto, T.; Kuwabata, S.; Sakata, T.; Mori, H.; Yoneyama, H. *Langmuir* **1995,** 11, 3725.

(7) Domen, K.; Sakata, Y.; Kudo, A.; Maruya, K.; Onishi, T. *Bull. Chem. Soc. Jpn* **1988,** 61, 359.

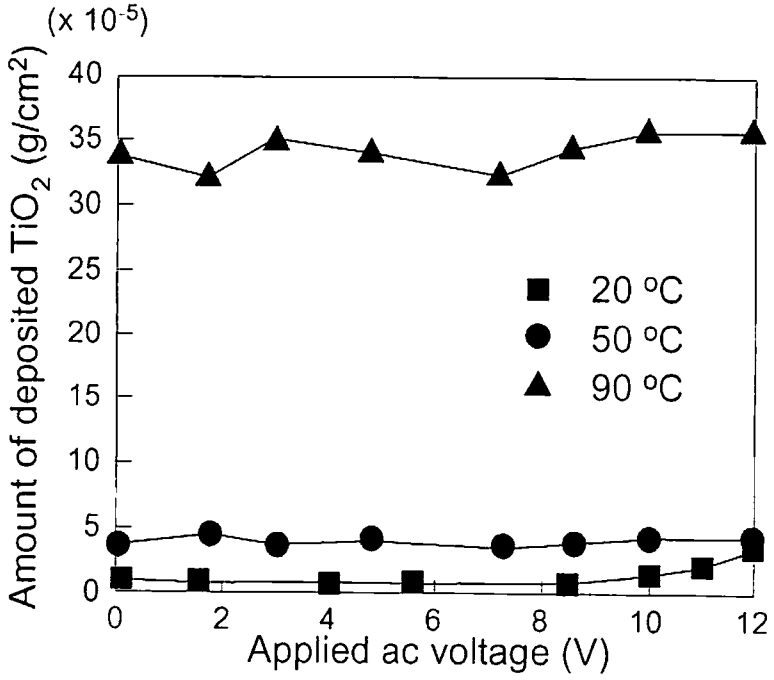

Fig. 4. 1. Amount of deposited TiO_2 as a function of the applied maximum ac voltage at various temperatures.

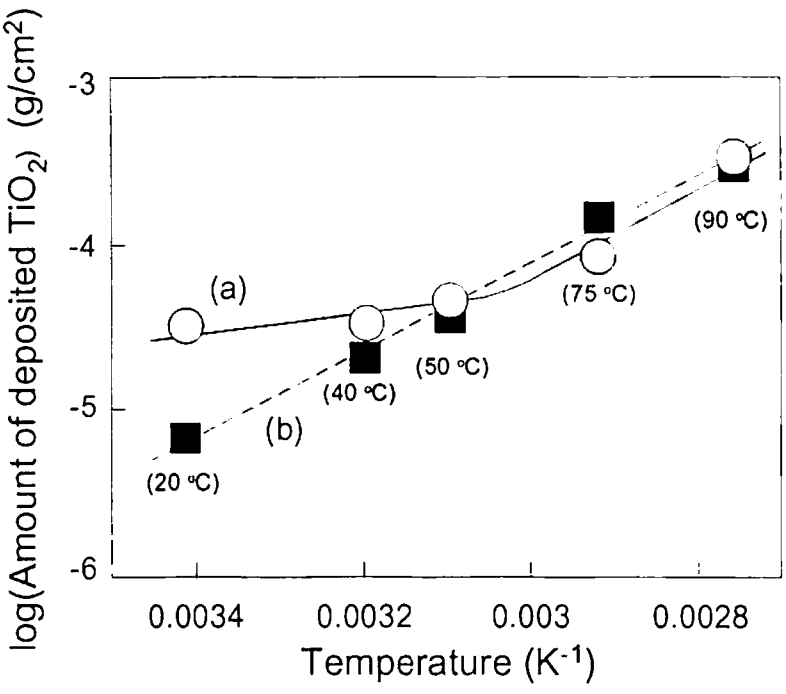

Fig. 4. 2. Arrhenius plot of the amount of deposited TiO_2 for the (a) applied ac 12 V and (b) nonapplied ac voltage.

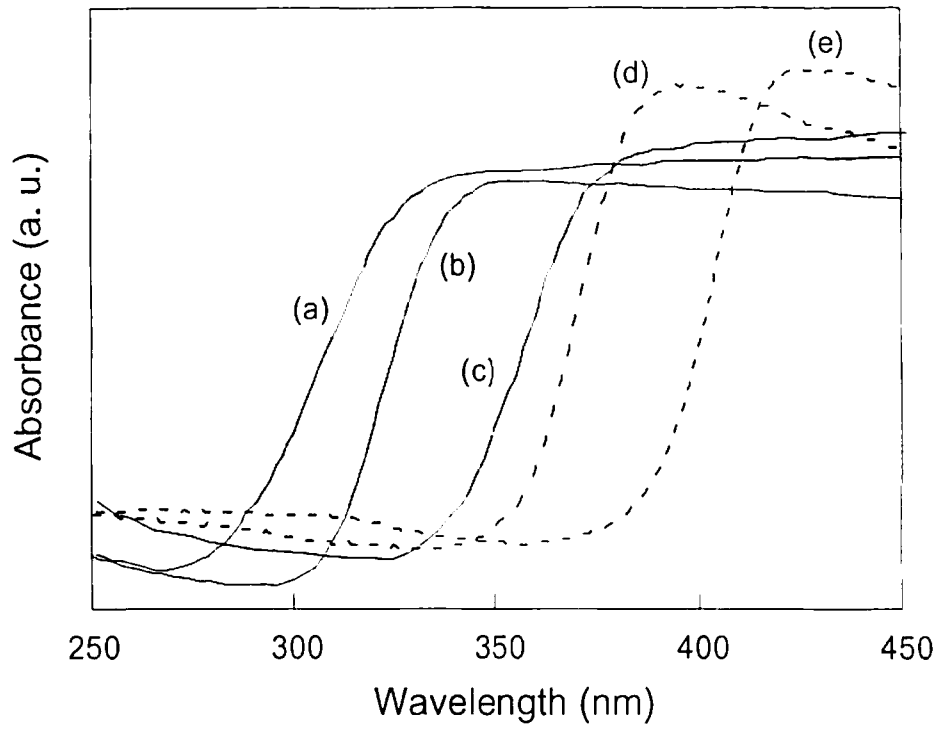

Fig. 4. 3. Absorption spectra of Al/Hard-Al_2O_3/TiO_2 prepared at ac 12 V for various temperatures and other TiO_2: (a) 20 °C, (b) 50 °C, (c) 90 °C, (d) anatase powder (0.3 μm), and (e) rutile powder (0.3 μm).

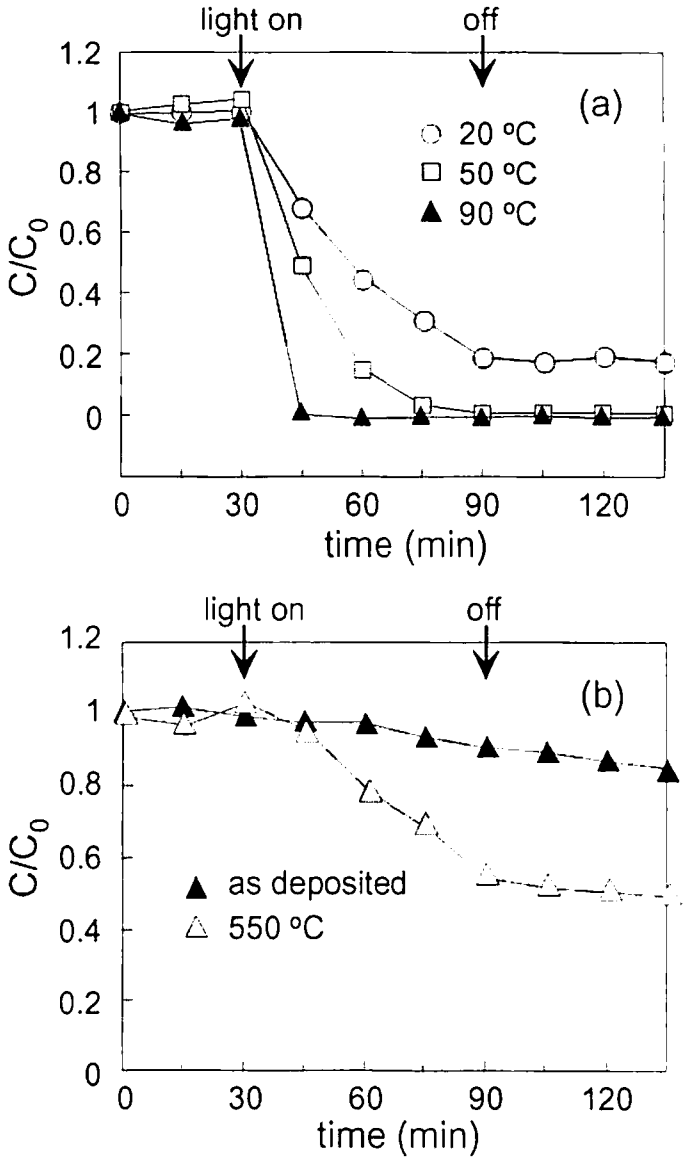

Fig. 4. 4. C (concentration)/C_0 [initial concentration, (a) 30 ppm, (b) 10 ppm] as a function of the illumination time, irradiated (a) by the xenon lamp and (b) and by the F-lamp.

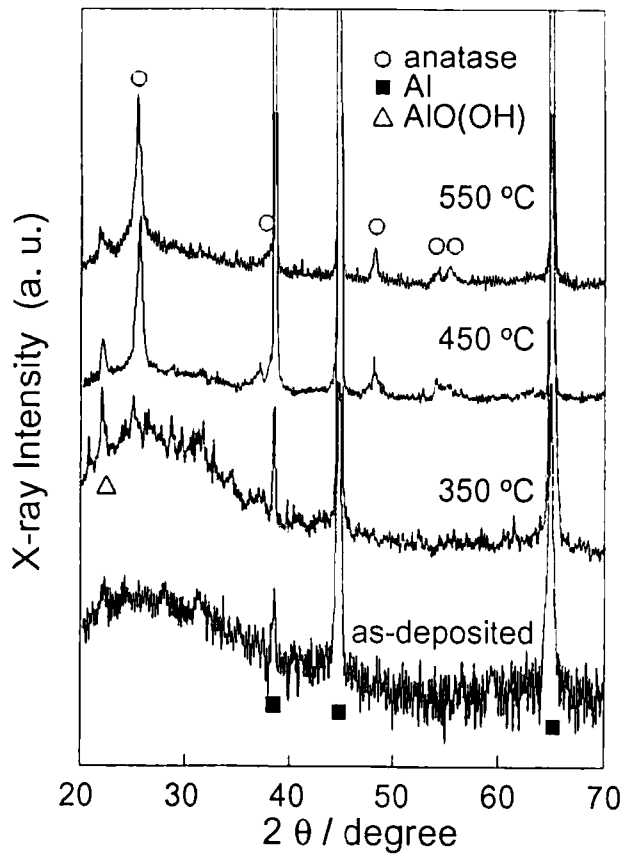

Fig. 4. 5. XRD patterns of the Al/Hard-Al_2O_3/TiO_2 heated at various temperatures, which were prepared at lower than 12 V and 90 °C.

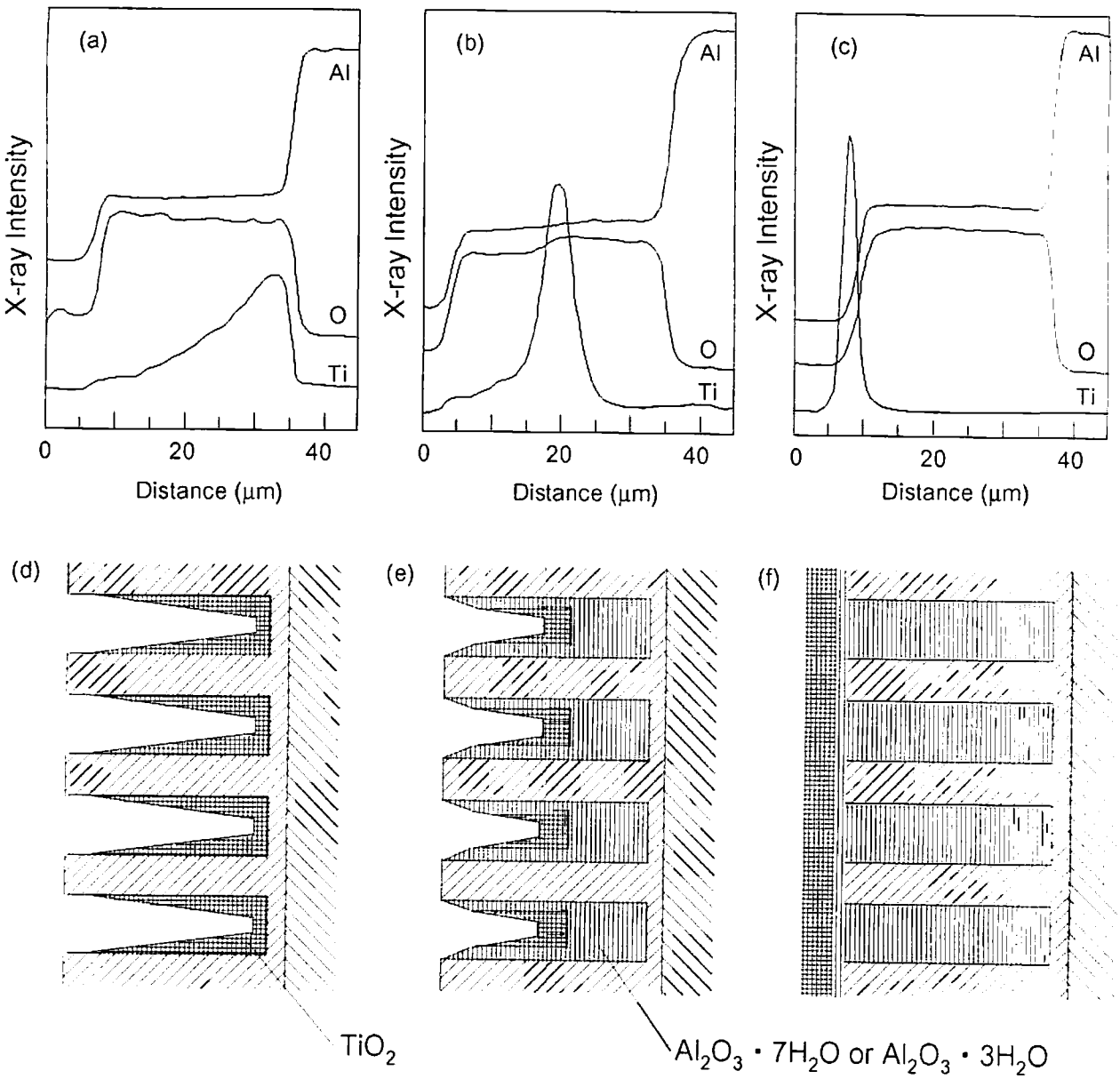

Fig. 4. 6. Line profile of EPMA elemental distribution in cross section of the Al/Hard-Al_2O_3/TiO_2 at ac 12 V and various temperatures: (a) 20 °C, (b) 50 °C, (c) 90 °C, and each model (d), (e), (f), respectively.

Chapter 5

Electrodeposition of TiO_2 into Porous Alumite Prepared in Phosphoric Acid

5. 1 Introduction

In chapter 2, we have demonstrated that a TiO_2 film with excellent photocatalytic activity was prepared and fixed onto alumtite by the electrodeposition technique consisting of two-step electrolysis.[1] However, the adhesion strengths in the interface of the Al_2O_3 (alumite)/TiO_2 as well as Al/Al_2O_3 was insufficient for practical use in this case. On the other hand, the one-step electrolysis in $(NH_4)_2[TiO(C_2O_4)_2]$ solution resulted in a thin TiO_2 film deposited uniformly in the pore of alumite and strong adhesion in the above interfaces, although the deposited TiO_2 showed low photocatalytic activity as stated in chapter 2.[1] The low photocatalytic activity is based on small amounts of the electrodeposited TiO_2 on the alumite prepared in sufuric acid solution, because the barrier layer is relatively thin (~60 Å) and broken by excess ac voltage and long time of electrolysis. In this study, TiO_2 deposition onto the alumite formed in phosphoric acid solution, which has relatively thick barrier later (~770 Å), was examined and its photocatalytic activity was evaluated.

5. 2 Experimental

An aluminum plate (60 x 50 mm, thickness 0.1 mm) was etched by immersion in alkaline solution and then electrochemically oxidized under 75 V in H_3PO_4 solution (0.001 M) for 4 h at 2 °C to prepare the porous alumite on its surface (Al/Al_2O_3). TiO_2 was electrodeposited by alternative electrolysis into pores of alumite ($Al/Al_2O_3/TiO_2$) prepared by the previous method. The electrolysis was carried out in a mixed aqueous solution consisting of 10^{-2} M $(NH_4)_2[TiO(C_2O_4)_2]$ and 2.5 x 10^{-3} M $(COOH)_2$ adjusted to pH 4 by titration with NH_4OH, under an ac bias at 293 K for 10 min. The graphite plate

(50 x 60 mm thickness: 10 mm) was used as the counter electrode, and the distance between the counter and working electrodes was fixed at 50 mm.

The elemental distribution of the prepared $Al/Al_2O_3/TiO_2$ was observed using electron probe microanalysis (EPMA). The pore diameter of the prepared alumite was approximately 100 nm by scanning electron microscope (SEM). The amount of deposited TiO_2 was analyzed by inductively coupled plasma (ICP) spectroscopy, where the sample was dissolved with 1.2 M H_2SO_4 and then the solution was analyzed. The UV and visible absorption spectrum of the $Al/Al_2O_3/TiO_2$ and anatase (99.9 %, Wako, Ltd.) and rutile TiO_2 (99.9 %, Wako, Ltd.) were measured with a UV/VIS spectrophotometer.

The photocatalytic activity of the prepared $Al/Al_2O_3/TiO_2$ was measured for the photodecomposition of acetaldehyde. A small amount of acetaldehyde gas was injected into a 1000 ml cylindrical quartz cell (62.5 cm^2 x 16 cm; the concentration was about 100 ppm), where the $Al/Al_2O_3/TiO_2$ was fixed in the cell in advance, and then illuminated. A 500 W xenon lamp (200 mW/cm^2) was used as the light source.

5. 3 Results and discussion

Figure 5. 1 shows the amount of TiO_2 deposited in the pores of the alumite after 10 minutes as a function of the applied maximum ac voltage. Most of the voltage was applied to the alumite during the electrolysis because of low resistance of the electrolyte (14.57 mS/cm). The amount of TiO_2 in the $Al/Al_2O_3/TiO_2$ was about 0.3 x 10^{-5} g/cm^2 in the ac voltage region less than about 70 V. However, this amount increased with the increase in the ac voltage region of more than 80 V. When the applied voltage exceeded about 100 V, the alumite was exfoliated from the aluminum substrate and therefore the amount of TiO_2 was decreased. In this case, TiO_2 deposition occurred

directly on the aluminum metal surface. Consequently, 90~100 V was the most suitable condition in the present electrolysis, and the amount of the deposited TiO_2 (4.7×10^{-5} g/cm^2) was much higher than that in the case of the one-step electrodeposition onto the alumite prepared in sulfuric acid solution (2.0×10^{-5} g/cm^2).

The electrodeposition of the $Al/Al_2O_3/TiO_2$ by the ac electrolysis will occur in the pores of the alumite during the cathodic process as follows:

$(NH_4)_2[TiO(C_2O_4)_2] \rightarrow TiO(C_2O_4)_2^{2-} + 2NH_4^+$ (1)

$2H_2O + 2e^- \rightarrow H_2$ (and/or $2H_{ads}$) $+ 2OH^-$ (2)

$TiO(C_2O_4)_2^{2-} + 2OH^- \rightarrow TiO_2 + H_2O + 2(C_2O_4)^{2-}$ (3)

$(NH_4)_2[TiO(C_2O_4)_2]$ will dissolve and then dissociate into $TiO(C_2O_4)_2^{2-}$ and ammonium ions (1) in aqueous solution before the electrolysis. Cathodic bias during the ac electrolysis brings about an electrochemical reaction (2) where OH^- ion is produced. Finally, TiO_2 (which will be somewhat hydrated) was produced in the pores of the alumite (3). The electrodeposition model is illustrated in Figure 5. 2. The above reactions were confirmed by the following experimental results. TiO_2 was precipitated in the solution when the pH of the solution containing $(NH_4)_2[TiO(C_2O_4)_2]$ was adjusted to about 5 from 4 by titration of the NH_4OH solution. Moreover, TiO_2 was deposited onto a Pt electrode by cathodic bias during dc electrolysis in the $(NH_4)_2[TiO(C_2O_4)_2]$ aqueous solution, but not anodic bias. Nevertheless, the ac electrolysis was necessary for the deposition of the TiO_2 in the pores of the alumite. Probably, the diffusion of $TiO(C_2O_4)_2^{2-}$ into the pores of alumite will totally increase under the ac bias, leading to the deposition of the TiO_2 in the pores in alumite as is well-known.[2] For the alumite formed in phosphoric acid solution, the applied ac voltage (90~100 V) to form TiO_2 was high compared with the case of the alumite formed in sulfuric acid solution whose thickness of the alumite layer is ca. 5-6 μm (8 V, as stated in chapter 2), since the barrier layer of the alumite formed in phosphoric acid solution (770 Å) is thicker than

that of the alumite formed in sulfuric acid solution (60 Å).[2]

The absorption spectra of the present TiO_2 deposited on alumite and other TiO_2 samples (anatase and rutile powder: 0.3 μm average particle size), are shown in Figure 5. 3. The deposited TiO_2 ((a), (b)) showed absorption in the wavelength region shorter than about 350 nm. Thus, relatively blue shifts were observed for the deposited TiO_2 ((a), (b)) compared with the anatase (c) and rutile (d) powders. A similar blue shift has already been observed for the quantized TiO_2 particles and/or highly dispersed TiO_2 in the porous substrate.[3-7] The blue shift in the deposited TiO_2 is probably due to the nano-sized TiO_2 in the pores of alumite. According to a calculation, the particle size of the deposite TiO_2 was less than 1 nm in radius in the case of 90 and 98 V electrolysis, respectively.[8]

Figure 5. 4 shows the SEM images of the alumite surfaces before (a) and after (b) the TiO_2 deposition at 98 V. The surface of the alumite scarcely changed by the TiO_2 deposition. Figure 5. 5 (a) shows the line profile of the EPMA elemental distribution in the cross section of the prepared $Al/Al_2O_3/TiO_2$. The part where Al overlaps with O in the distribution corresponds to the alumite film formed on the Al substrate, the thickness of the alumite layer is estimated to be about 4-5 μm. From this figure, it was found that TiO_2 was mainly deposited near the middle point in the pores.

The adhesion strength of the interfaces of the Al_2O_3/TiO_2 and Al/Al_2O_3 was insufficient in the case of two-step electrolysis as reported in chapter 2.[1] This is based on the presence of the deposited TiO_2 mainly on the surface of alumite in the case of Al_2O_3/TiO_2 interface. On the other hand, the TiO_2 deposited by the present one-step electrolysis existed in the pore of alumite as described above, leading to strong adhesion. In practice, most of the TiO_2 deposited by the two-step electrolysis was removed from the alumite, but not for the present case of the one-step electrolysis, according to a Scotchtape adhesion peel test. Consequently, an improvement of the adhesion of the

interfaces of the Al_2O_3/TiO_2 and Al/Al_2O_3 was accomplished by the present one-step electrolysis.

According to the EPMA elemental distribution, Ti exists on the walls of the pores and the expected model is shown in Fig. 5. 5 (b). A few Ti species are adsorbed on the wall of the pore with positive charge by an electric force, because the Ti species will exist as anion (1) in $(NH_4)_2[TiO(C_2O_4)_2]$ aqueous solution at pH 4.0 (The PZC of alumite is pH=8.[9]). Consequently, it is suggested that the adsorbed Ti species changed to TiO_2 on the wall by the pH increase during the process, as shown in Figure 5. 2. The total amount of deposited TiO_2 in one pore in the alumite which was prepared at 98 V was estimated from the amount of TiO_2 analyzed by ICP measurement to be 1.3×10^{-14} g, where the number of pores of the present alumite is assumed to be 3.6×10^9 /cm^2 from SEM image (Fig. 5. 4 (a)). If the deposited TiO_2 exists with 100 % density as anatase or rutile phase in the pore walls, the average thickness of the TiO_2 was estimated to be less than about 2 nm. No diffraction peak in XRD measurement was observed even for the heat-treated TiO_2 at 500 °C, because the amount of deposited TiO_2 in the pores of alumite is too small to be detected. Moreover, no Raman peak due to anatase and rutile phase was observed for the deposited TiO_2. This will be due to the nano-sized TiO_2 as well as its small amount.

Figure 5. 6 shows the concentration of acetaldehyde as a function of illumination time for the $Al/Al_2O_3/TiO_2$ samples prepared on the alumite formed in phosphoric acid solution. In this figure, the $Al/Al_2O_3/TiO_2$ sample prepared by the one-step electrodeposition at 8 V on the alumite in sulfuric acid (as stated in chapter 2) for comparison. The concentration gradually decreased with illumination for each sample, indicating that all the deposited TiO_2 in the alumite pores has photocatalytic activity. The apparent photocatalytic activity is increased with the increase in the applied ac voltage in the case of the alumite prepared in phosphoric acid solution, because the

amount of the TiO_2 increased with the applied ac voltage.

5. 4 Conclusions

In conclusion, the one-step electrodeposition of TiO_2 photocatalyst into the pores of alumite formed in phosphoric acid solution succeeded using an ac electrolysis technique. The TiO_2 was deposited by an increase in the pH in the pores in the cathodic process during high voltage ac electrolysis compared with that in the case of the alumite prepared in sulfuric acid solution. The adhesion of the interfaces of the Al/Al_2O_3 and Al_2O_3/TiO_2 was improved by the present one-step electrolysis, because the TiO_2 deposited on the pores walls. The deposited TiO_2 in the pore of alumite formed in phosphoric acid solution shows high photocatalytic activity compared with that of the deposited TiO_2 on the alumite formed in sulfuric acid solution. This will be mainly due to the relatively large amount of deposited TiO_2.

References

(1) Matsumoto, Y.; Ishikawa, Y.; Nishida, M.; Ii, S. *J. Phys. Chem. B* **2000,** 104, 4202.

(2) Mita, I.; Kuroda, K.; Suzuki, K.; Muramatsu, Y.; Nemoto, S.; Yamada, M.; *Handbook of Aluminium Surface Treatment*; Light Metal Publishing: Tokyo, 1980.

(3) Anpo, M.; Aikawa, N.; Kubokawa, Y.; Che, M.; Louis, C.; Giamello, E. *J. Phys. Chem.* **1985,** 89, 5017.

(4) Liu, X.; Lu, K. K.; Thomas, J. K. *J. Chem. Soc., Faraday Trans.* **1993,** 89, 1861.

(5) Uchida, H.; Hirao, S.; Torimoto, T.; Kuwabata, S.; Sakata, T.; Mori, H.; Yoneyama, H. *Langmuir* **1995,** 11, 3725.

(6) Domen, K.; Sakata, Y.; Kudo, A.; Murayama, K.; Ohishi, T. *Bull. Chem. Soc. Jpn.* **1988,** 61, 359.

(7) Yamashita, H.; Ichihashi, Y.; Anpo, M.; Hashimoto, M.; Louis, C.; Che, M. *J. Phys. Chem.* **1996,** 100, 16041.

(8) Goossens, A. *Surf. Sci.* **1997,** 371, 390.

(9) Xiong, G.; Feng, Z.; Li, J.; Yang, Q.; Ying, P.; Xin, Q.; Li, C. *J. Phys. Chem. B* **2000,** 104, 3581.

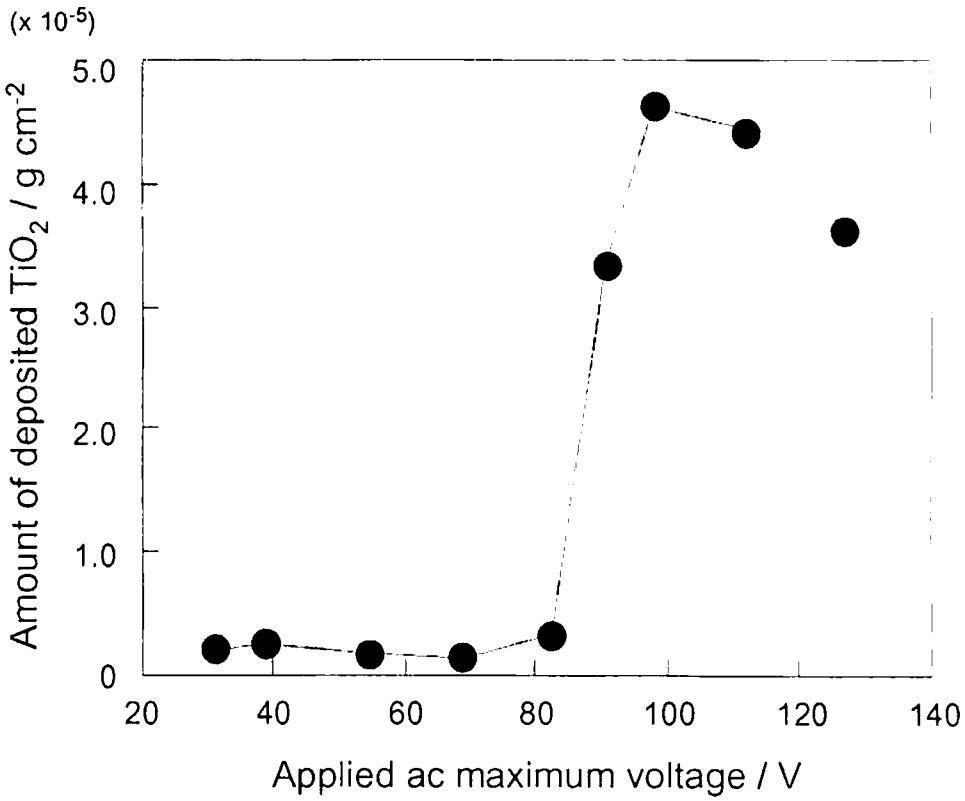

Fig. 5. 1. Amount of deposited TiO_2 as a function of applied ac voltage.

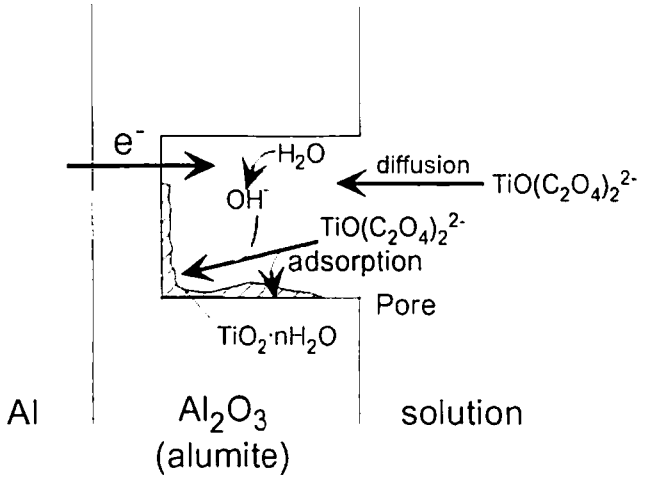

Fig. 5. 2. Model of the electrodeposition mechanism for the $Al/Al_2O_3/TiO_2$.

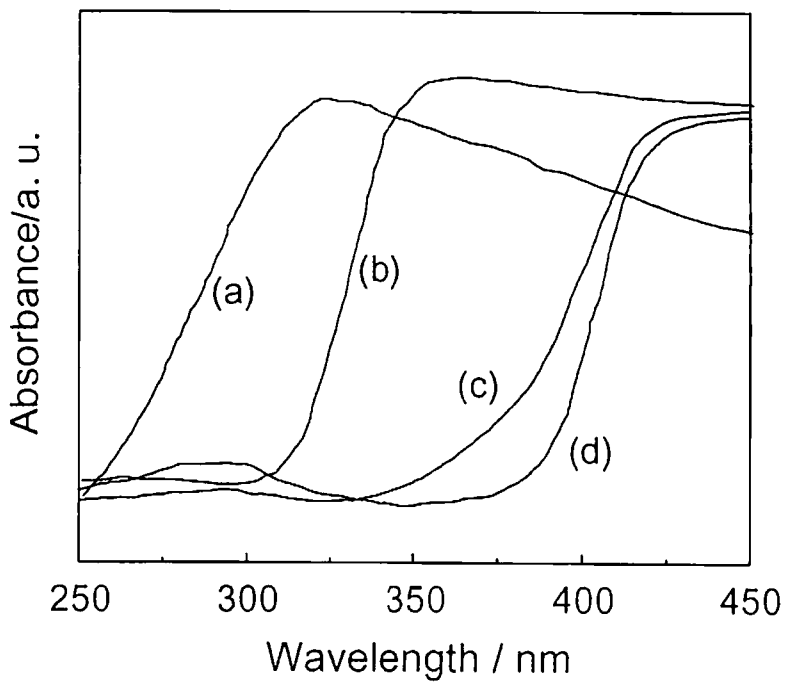

Fig. 5. 3. Absorption spectra of $Al/Al_2O_3/TiO_2$ prepared at 90 V (a), 90 V (b), anatase powder (0.3 μm) (c), and rutile powder (0.3 μm) (d).

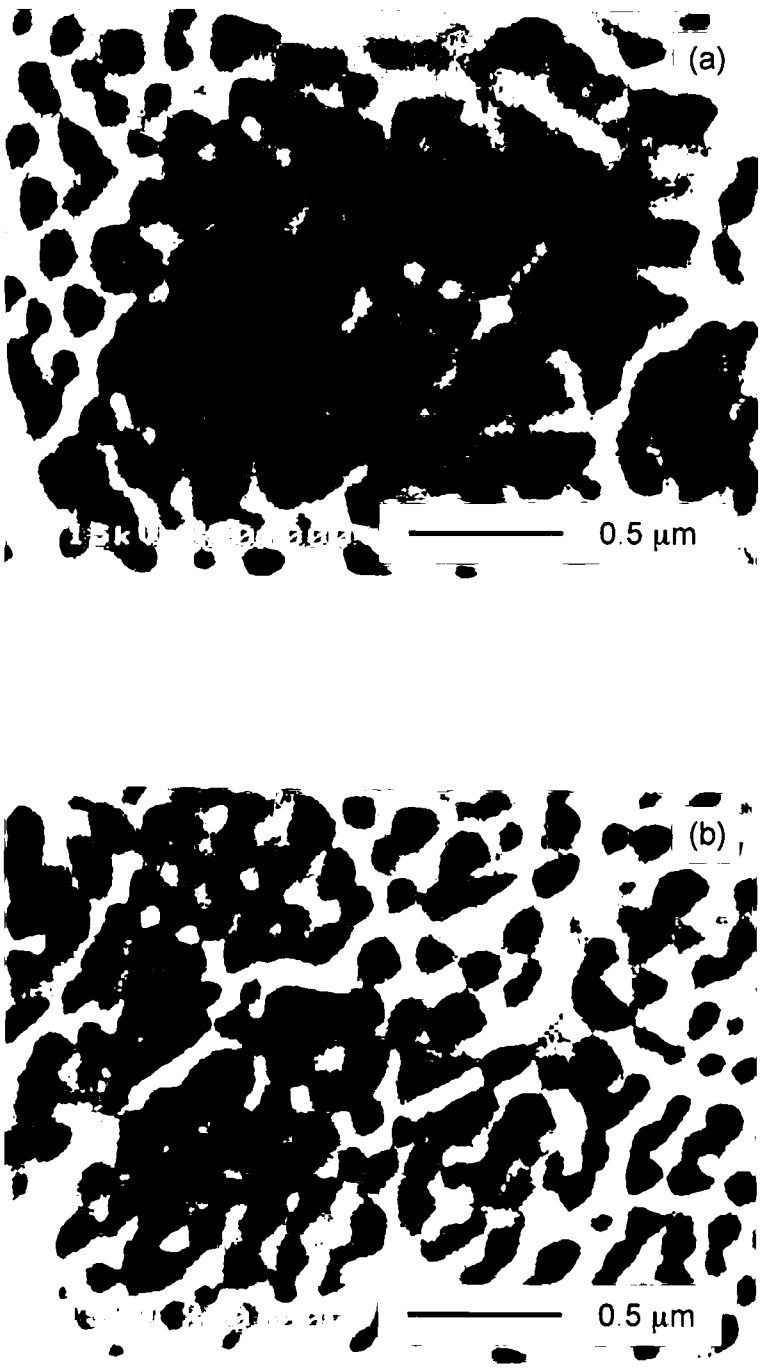

Fig. 5. 4. SEM images of the alumite surface (a) before TiO_2 deposition and (b) deposited TiO_2 at 98 V.

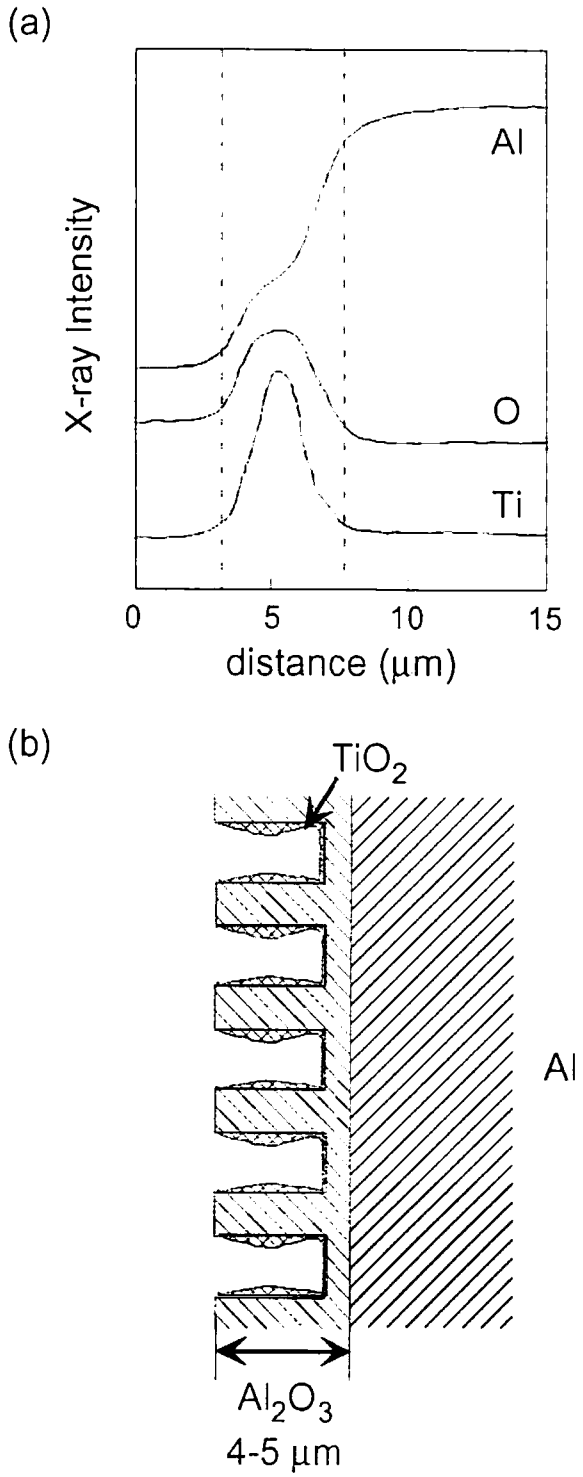

Fig. 5. 5 Line profile of EPMA elemental distribution in cross section of the $Al/Al_2O_3/TiO_2$ at ac 98 V (a) and its model (b).

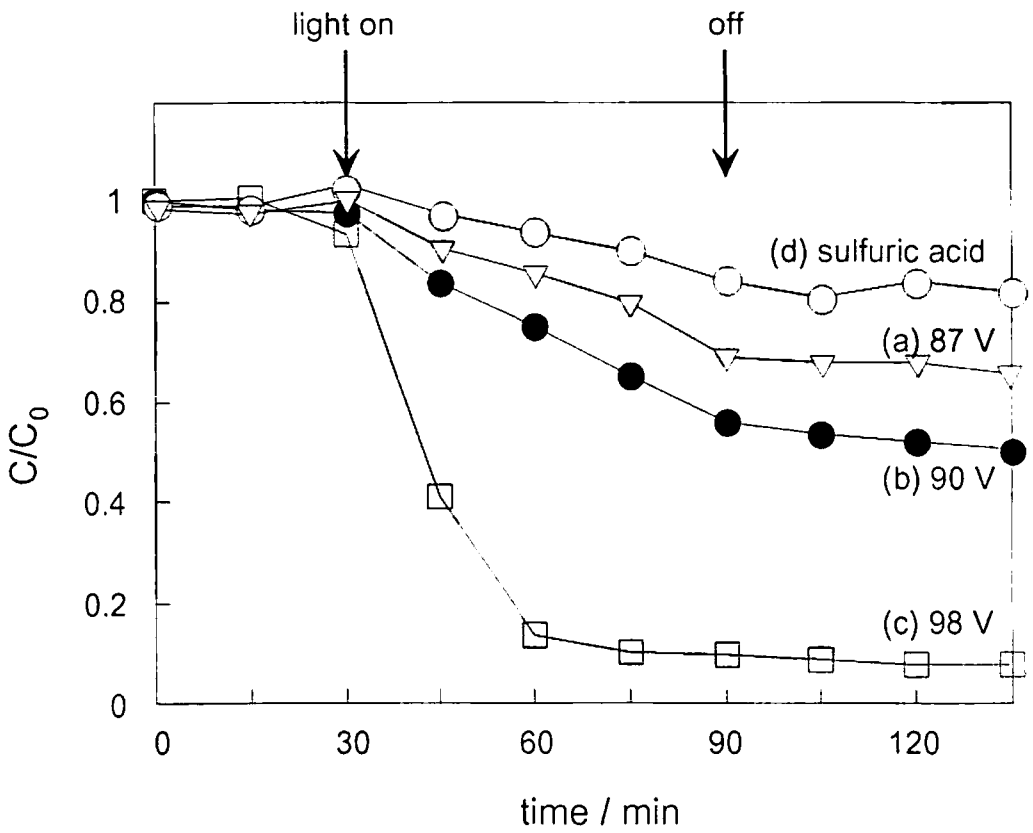

Fig. 5. 6. C (concentration)/C_0 (initial concentration, ca. 100 ppm) as a function of illumination time. The alumite formed in phosphoric acid solution deposited TiO_2 at 87 V (a), 90 V (b), 98 V (c), and the alumite formed in sulfuric acid solution deposited TiO_2 at 6 V (d).

Chapter 6

Surface Treatment of SiC and Diamond Using Titanium(IV) Oxide Photocatalyst

6. 1 Introduction

Silicon carbide (SiC) and diamond are well-known as abrasive materials for grinding and polishing because of their excellent hardness. Moreover, they can also be used in the near future as semiconductor materials with a wide-bandgap, which is very useful as some power devices.[1-7] Thus, SiC and diamond are promising materials in the precision machining and electrical industries. The surface treatment of these materials such as chemical modification in-area and in-depth and/or nano-and micro-level etching, will be very important for developing the production of micro-machines and micro-devices.[4,8-16] In general, chemical modification such as etching and oxide formation are made by laser beam ablation and/or thermal oxidation at high temperature.[1,2,12,13] On the other hand, polishing these materials is done with some fine particles such as diamond that have excellent hardness.[4,17,18] However, the surface treatments of SiC and diamond are very difficult under mild conditions that are necessary for the film-type fabricated devices.[20,21] We now show that the surfaces of silicon carbide (SiC) and diamond with hard and chemically stable properties can be photocatalytically decomposed and modified using a TiO_2 photocatalyst. The SiC surface is decomposed to CO_2 and SiO_2 on its surface by the photocatalysis of TiO_2 under illumination at room temperature. The diamond is also decomposed to CO_2. This technique using the TiO_2 photocatalyst will be very useful as a nano-level surface treatment such as a photo-patterning under mild conditions for SiC and diamond.

6. 2 Experimental

Photocatalytic decomposition test of SiC and diamond powders by the TiO_2

photocatalysis

SiC (Nacalai Tesque Co., Ltd., 200 μm average particle size, 0.026 m^2 g^{-1} BET surface area) and diamond (Engis Co., Ltd., 0.25 μm average particle size, 20 m^2 g^{-1} BET surface area) powders were used as the reactant for the photocatalytic decomposition test. TiO_2 powder (Degussa Co., Ltd., 30 nm average particle size) consisting of anatase (80 %) and rutile (20 %) was used as the photocatalyst in this study. The TiO_2 powder was irradiated with a 500 W Hg-lamp for 10 h before the above decomposition test so that any organic compound absorbed on the surface of the TiO_2 powder was decomposed. The TiO_2 (1 g) and the SiC or diamond (1 g) were mixed, and then placed in a quartz vessel (1 L) filled with air. Light from the 500 W Hg-lamp was illuminated to the mixed powder. The produced CO_2 was analyzed by gas chromatography (TCD). Two types of the surface modified diamond powder were used in this study. One had a C-O bond on the surface, which was produced by immersion in H_2SO_4-HNO_3 (9:1 v/v) solution at 80 °C for 4 h. The other had a C-H bond on the surface, which was produced by preheat-treatment in H_2 at 900 °C for 5 h. The presence of C-H or C-O bonds on the diamond surface was confirmed by FT-IR measurements.

Surface treatment test of SiC substrate by the TiO_2 photocatalysis

A 3C-SiC single crystal (111) (3 x 5 x 1 mm^3) was used as the substrate to study the surface treatment using the TiO_2 photocatalysis. The SiC single crystal was etched by immersion in a HF aqueous solution to remove the surface oxide. A quartz plate coated with a transparent TiO_2 film (0.5 μm thickness), which was prepared by spin-coating at ~2000 rpm using TiO_2 sol (Nippon Soda Co., Ltd., NDC-100C, particle size of about 10 nm), was attached to the surface of the SiC single crystal, and then irradiated by the 500 W Hg-lamp, as shown in Fig. 6. 1. The surface of the SiC single crystal after illumination was analyzed by X-ray photoelectron spectroscopy (XPS).

A photo-patterning test was carried out using the surface of the SiC single crystal. The quartz plate surface coated with the TiO_2 film was attached to the SiC single crystal. An aluminum plate with a hole (0.5 mm thickness, 1.5 mm Φ) was placed on the other side of the quartz surface during the photo-patterning test (see Fig. 6. 8 (a)). The illumination was done using the 500 W Hg-lamp.

Remote surface treatment test for the SiC substrate by air/H_2O flowing system

A quartz tube (150 mm length, ϕ 18 mm) was packed with many quartz beads (ϕ 2 mm) coated with the TiO_2 film, and then air with various humidity was flowed into the tube with flowing rate of 1.5 L/min. The 3C-SiC single crystal was placed at the position of 3 mm apart from the outlet, as shown in Fig. 6. 2. The SiC surface as well as the tube were illuminated by the 500 W Hg-lamp for 6 h unless otherwise stated. The surface of the SiC single crystal after the test was analyzed by XPS.

6. 3 Results and Discussion

Results and Discussion

6. 3. 1 Photocatalytic decomposition of SiC and diamond powders by the TiO_2 photocatalysis.

Figure 6. 3 shows the concentration of produced CO_2 in the vessel as a function of illumination time when the SiC powder was used as the reactant. CO_2 was produced in the case of the SiC/TiO_2 powder mixture, but not for the SiC powder without TiO_2 and the mixture in the dark or under illumination of light with wavelengths longer than about 440 nm, indicating that the TiO_2 photocatalytically decomposes the SiC to CO_2. The production rate of CO_2 from the SiC/TiO_2 powder mixture decreased in the cases of the illumination times longer than about 30 min, suggesting that the SiC surface changed to SiO_2 by the photocatalytic oxidation. This was confirmed by the XPS

measurement as stated in a later section. No CO_2 was produced for the mixture after a 10 h illumination, as shown in Fig. 6. 3, since the surfaces of the SiC particles were covered with the SiO_2. It was estimated that about 1.7 x 10^{-6} mol of CO_2 was produced in the case of the SiC /TiO_2 powder mixture illuminated for 30 min. The amount of the surface C atom on SiC is estimated to be about 1.2 x 10^{-5} mol m^{-2}, if the decomposition surface is assumed to be the (110) plane (The cleavage plane of SiC is (110).). The total amount of the surface C atom is calculated to about 3.2 x 10^{-7} mol g^{-1} in the present test (SiC 1 g), because the SiC powder used in this study had a specific surface area of 0.026 m^2 g^{-1}. Consequently, it is concluded that about 530 % of the surface C atoms is decomposed to CO_2 after 30 min illumination.

Figure 6. 4 shows the concentration of the produced CO_2 in the vessel as a function of illumination time when the diamond powder was used as the reactant. CO_2 was produced in the case of the diamond/TiO_2 powder mixture, but not for the diamond powder without TiO_2 and the TiO_2 powder without diamond powder even under illumination. No CO_2 was produced for the mixtures in the dark or under the illumination of light with wavelengths longer than about 440 nm. Thus, the surface of diamond was also photocatalytically oxidized to CO_2 by the TiO_2 photocatalysis. The photocatalytic decomposition of diamond occurred on both the surfaces with C-H and C-O bonds, indicating that the photocatalytic decomposition of diamond does not depend on its surface composition. About 7.7 x 10^{-6} mol of CO_2 was produced in the case of the diamond /TiO_2 powder mixture illuminated for 2 h. The amount of the surface C atom on diamond was estimated to be 3.0 x 10^{-5} mol m^{-2}, if the decomposition surface is assumed to be the (111) plane (The cleavage plane of diamond is (111).). The total amount of the surface C atom was calculated to be about 6.0 x 10^{-4} mol g^{-1}, because the diamond powder used in this study (diamond 1 g) had a specific surface area of 20 m^2 g^{-1}. Consequently, it is concluded that only about 1 % of the surface C atom of the

diamond powder is decomposed to CO_2 after 2 h illumination. Both surfaces of the (100) plane of the single crystal and a CVD polycrystalline diamond (Sumitomo Electric Industries, Ltd., 5 x 5 x 0.5 mm^3) were scarcely etched under illumination for 200 h using the same system as Fig. 6. 1, according to an atomic force microscope (AFM) observation. This is due to the slow photocatalytic decomposition rate of diamond as stated above. Probably, more intense light may be necessary for the clear photo-patterning of diamond surface.

6. 3. 2 Surface treatment of SiC substrate by the TiO_2 photocatalysis.

Figure 6. 5 shows the XPS spectra of Si2p of the SiC surface after various treatments for 1 h, where the surface treatment system of Fig. 6. 1 was used. Si^{4+} was observed at the SiC surface in contact with the TiO_2 film after illumination (a), but not for that without illumination (b). The same spectrum as for the case (b) was obtained for the illumination of light with wavelengths longer than about 440 nm (c). In the case of the illumination without TiO_2 (d), a slight Si^{4+} was observed. This case may be due to the surface oxidation by active oxygen and/or O_3 produced by UV irradiated air.[3] For the illumination with TiO_2 (a), the atomic ratio of O/Si^{4+} on the surface was about 2 according to the XPS analysis, indicating that SiO_2 is formed during the photocatalytic reaction.

An aluminum metal film, whose thickness was about 15 μm, was placed between the quartz plate coated with the TiO_2 film and the SiC substrate in order to keep a space (gap distance: 15 μm) between the TiO_2 film and the SiC surface (non-contact), as shown in Fig. 6. 6 (a). Figure 6. 6 (b) shows the XPS spectra of Si2p of the SiC surface after the illumination for 1 h. Si^{4+} was observed at the window, but not under the Al film, indicating that SiO_2 was formed on the surface of the SiC by the photocatalytic oxidation even under the condition of non-contact with the TiO_2.

Two mechanisms for the TiO_2 photocatalytic oxidation of chemical compounds have been reported. One mechanism is a direct oxidation of the reactant by the photo-generated hole in the valence band. The other is the oxidation of the reactant by some active oxygen species such as $OH^{\cdot}$, $HO_2^{\cdot}$, $O_2^{\cdot-}$, H_2O_2 and $^1O_2$ produced by the reaction between H_2O and/or O_2 and the hole. In the photocatalytic oxidation of the SiC, the latter oxidation by the active oxygen species will preferentially occur, because SiO_2 was formed even under the condition of non-contact with the TiO_2 as stated above. Tatsuma et al.[22] reported that aromatic and aliphatic substances were oxygenated and oxidized to CO_2 by the non-contact photocatalysis (gap distance: 50 μm-2.2 mm). They explain that photo-generated $OH^{\cdot}$ and $HO_2^{\cdot}$ on the surface of the TiO_2 will change to H_2O_2 at first stage as follows:

$$2HO^{\cdot} \rightarrow H_2O_2 \qquad (1)$$

$$2HO_2^{\cdot} \rightarrow H_2O_2 + O_2 \qquad (2)$$

Then the generated H_2O_2 will diffuse in the gas phase from the TiO_2 surface to the reactant surface, where the re-produced $OH^{\cdot}$(eq 3) under illumination oxidizes the reactact.[22]

$$H_2O_2 \xrightarrow{h\nu} 2OH^{\cdot} \qquad (3)$$

No oxidation of SiC to SiO_2 occurred by immersion of the SiC substrate in H_2O_2 (35%) for 6 h. On the other hand, the oxidation was observed, after the light was illuminated on the SiC surface during the H_2O_2 immersion. Moreover, the oxidation occurred by the Fenton reaction, where the H_2O_2 solution added with $FeSO_4$ was used as the immersion solution to produce $OH^{\cdot}$.[23] These results suggest that the SiC will be directly oxidized by $OH^{\cdot}$ as denoted by eq. (4). This is indirectly confirmed by the remote surface treatment test as stated in the later section.

$$SiC + 4OH^{\cdot} + O_2 \rightarrow SiO_2 + 2H_2O + CO_2\uparrow \qquad (4)$$

Figure 6. 7 shows the depth profiles of the XPS spectra of Si2p (a), C1s (b),

and O1s (c) of the SiC surface after the illumination for 1 h, where the same system as Fig. 6. 1 was used. By increasing the Ar etching time, the peak intensities of the $Si^{4+}2p$ (shown in (a)) and O1s (shown in (c)) decreased, whereas those of the $Si^{0+}2p$ (shown in (a)) and C1s (shown in (b)) increased. It was estimated from the $Si^{4+}2p$ depth profile that the thickness of the formed SiO_2 film is about 40 Å, since the etching rate was about 0.5 Å/sec. This thickness is roughly consistent with that calculated from the CO_2 production result.

Figure 6. 8 (a) shows the system for the photo-patterning test of the SiC. Fig. 6. 8 (b) and (c) show the mapping of the $Si^{4+}2p$ and O1s spectra on the SiC surface after the illumination respectively. From the comparison between the system (a) and the mapping (b) and (c), it is concluded that the photo-patterning of the SiO_2 formation on the SiC surface is easily accomplished by the TiO_2 photocatalysis.

6. 3. 3 Remote surface treatment for the SiC substrate by air/H_2O flowing system

Figure 6. 9 shows the XPS spectra of Si2p of the SiC surface treated by the remote surface treatment system (shown in Fig. 6. 2). Si^{4+} was observed on the SiC surface only in the cases of air with H_2O under the illumination ((a)-(c)). The degree of the oxidation increased with the increase of RH. No peak of $Si^{4+}2p$ was observed in the cases of dark, the quartz beads without TiO_2 under the illumination, and pure N_2 with H_2O under illumination to the quartz beads coated with TiO_2 (d). These results indicate that some active oxygen species photo-generated on the TiO_2 surface flow to the outlet of the tube and then oxidize the SiC surface, and that the most active oxygen species will be $OH^{\cdot}$ and/or $HO_2^{\cdot}$ produced from H_2O for the SiC oxidation. In this case, O_2 will act as a capture of the produced electron or as an oxidant for the oxidation of the SiC as denoted in eq. (4).

In this remote system, $OH^{\cdot}$ and/$HO_2^{\cdot}$ photo-generated at the TiO_2 surface will

not diffuse to the SiC surface, because these radicals are short in life time. Probably, H_2O_2 diffusion and radical re-production mechanism will be important as stated already, since the degree of the oxidation of the SiC surface largely decreased by the suppression of light illumination to the SiC surface in the present remote system (where the quartz beads coated with TiO_2 was illuminated). Consequently, the remote surface treatment system is that for the radical photo-generation using the TiO_2 photocatalysis. This system will be practically useful for the portable and moving surface treatments of the SiC and other materials under mild conditions, because the reactant surface and the TiO_2 photocatalyst is separated in position.

6. 4 Conclusions

In conclusion, CO_2 was produced by the TiO_2 photocatalytic decomposition of the SiC and diamond surfaces at room temperature. The TiO_2 photocatalysis brought about the SiO_2 formation on the SiC surface, and therefore, the surface photo-patterning. Thus, the TiO_2 photocatalysis will be useful for the surface treatment of the SiC surface without defects and sub-surface damage, because the reaction is carried out under mild conditions. The remote surface treatment system using the tube filled with the quartz beads coated with TiO_2 was also developed. This system confirmed that the $OH^{\cdot}$ significantly act as the oxidizing agent for the photocatalytic oxidation of the SiC surface. Moreover, this system will be practically useful for the surface treatment separating between the reactant surface and the TiO_2 photocatalyst.

References

(1) Raynaud, C. *J. Non-cryst. Solids* **2001,** 280, 1.

(2) Virojanadara, C.; Johansson, L. I. *Surf. Sci.* **2001,** 472, L145.

(3) Kosugi, R.; Ichimura, S.; Kurokawa, A.; Koike, K.; Fukuda, K; Suzuki, S.; Okushi, H.; Yoshida, S.; Arai, K. *Appl. Surf. Sci.* **2000,** 159-160, 550.

(4) Zhou, L.; Audurier, V.; Pirouz, P.; Anthony, P. J. *J. Electrochem. Soc.* **1997,** 144. L161.

(5) Diederich, L.; Küttel, O. M.; Ruffieux, P.: Pillo, Th.; Aebi, P.; Schlapbach, L. *Surf, Sci.* **1998,** 417, 41.

(6) Itahashi, M.; Umehara, Y.; Koide, Y.; Murakami, M. *Diamond Relat. Mater.* **2001,** 10, 2118.

(7) Corrigan, T. D.; Gruen, D. M.; Krauss, A. R.; Zapol, P.; Chang, R. P. H. *Diamond Rlat. Mater.* **2002,** 11, 43.

(8) Kiyohara, S.; Ayano, K.; Abe, T.; Mori, K. *Jpn. J. Appl. Phys.* **2000,** 39. 4532.

(9) Bail, E. S.; Baik, Y. J.; Jeon, D. *Diamond Relat. Mater.* **1999,** 8, 2169.

(10) Chen, Y. H.; Hu, C. T.; Lin, I. N. *Jpn. J. Appl. Phys.* **1997,** 36, 6900.

(11) Sandhu, G. S.; Chu, W. K. *Appl. Phys. Lett.* **1989,** 55, 437.

(12) Makhtari, A.; Raineri, V.; Via, L. F.; Franzó, G.; Frisina, F.; Calcagno, L. *Mater. Sci. Semicond. Process.* **2001,** 4, 345.

(13) Johnson, M. B.; Zvanut, M. E.; Richardson, O. *J. Electron. Mater.* **2000,** 29, 368.

(14) Strother, T.; Knickerbocker, T.; Russell, J. N. Jr.; Butler, J. E.; Smith, L. M.; Hamers, R. J. *Langmuir* **2002,** 18, 968.

(15) Kim, C. S.; Mowrey, R. C.; Butler, J. E.; Russell, J. N. Jr. *J. Phys. Chem. B* **1998,** 102, 9290.

(16) Miller, J. B.; Brown, D. W. *Langmuri* **1996,** 12, 5809.

(17) Grillo, S. E.; Field, J. E.; Van Bouwelen, F. M. *J. Phys. D: Appl. Phys.* **2000,** 33,

985.

(18) Van Bouwelen, F. M. *Phys. Stat. Sol. (a)* **1999,** 172, 91.

(19) Hirabayashi, K.; Taniguchi, Y.; Takamatsu, O.; Ikeda, T.; Ikoma, K.; Iwasaki, K. *Appl. Phys. Lett.* **1988,** 53, 1815.

(20) Chappel, D. C.; Smith, J. P.; Taylor, S.; Eccleston, W.; Das, M. K.; Cooper, J. A.; Melloch, M. R. *Electron. Letters,* **1997,** 33, 97.

(21) Kobayashi, H.; Sakurai, T.; Nishiyama, M.; Nishioka, Y. *Appl. Phys. Lett.* **2001,** 78, 2336.

(22) Tatsuma, T.; Tachibana, S.; Fujishima, A. *J. Phys. Chem. B* **2001,** 105, 6987.

(23) Fujihara, M.; Satho, Y.; Osa, T. *Bull. Chem. Soc. Jpn.* **1982,** 55, 666.

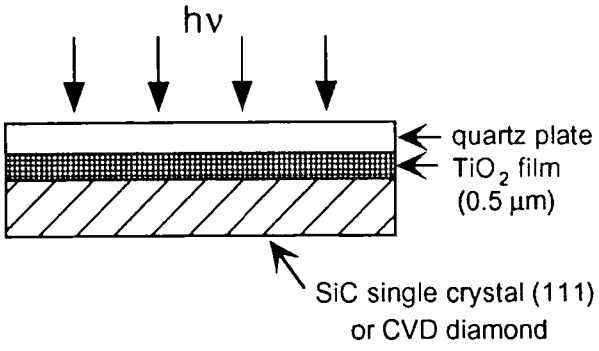

Fig. 6. 1. Model of surface treatment system for the SiC single crystal or CVD diamond.

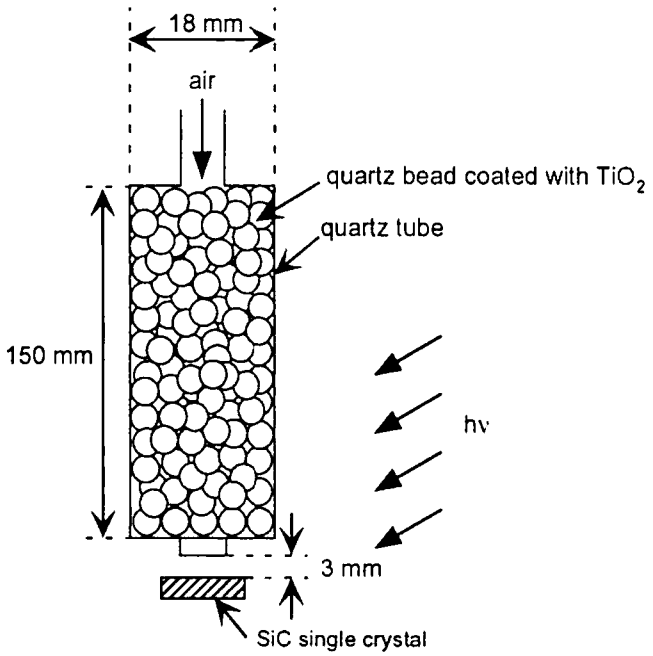

Fig. 6. 2. Model of the remote surface treatment system for the SiC single crystal surface.

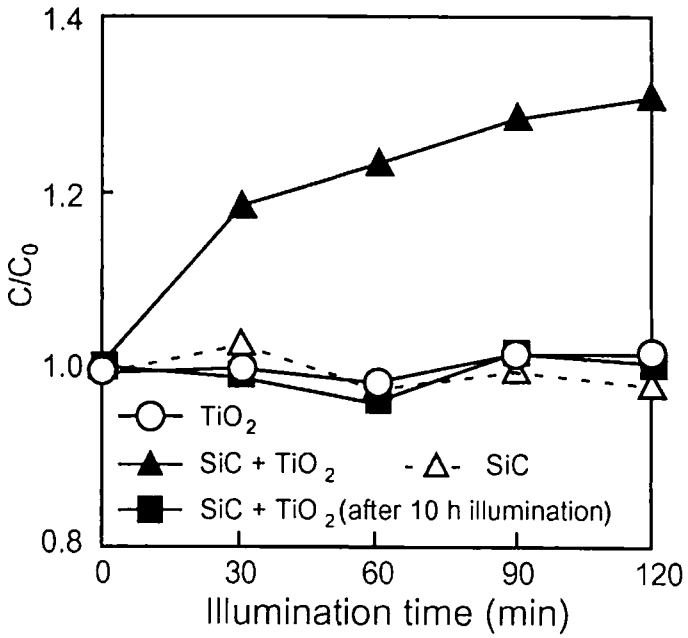

Fig. 6. 3. C (concentration)/C_0 (initial concentration, ca. 330 ppm) as a function of the illumination time for CO_2 produced in the quartz cell. The SiC powder was used as the reactant.

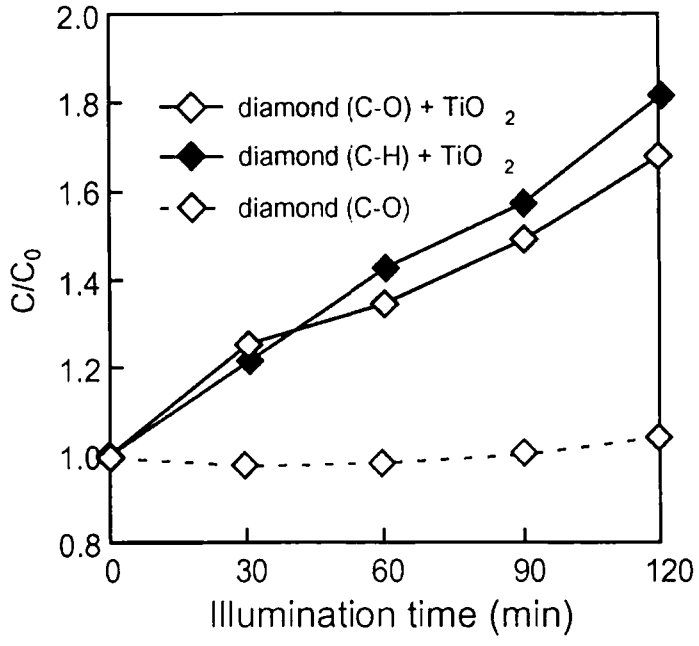

Fig. 6. 4. C (concentration)/C_0 (initial concentration, ca. 330 ppm) as a function of the illumination time for CO_2 produced in the quartz cell. The diamond powder was used as the reactant.

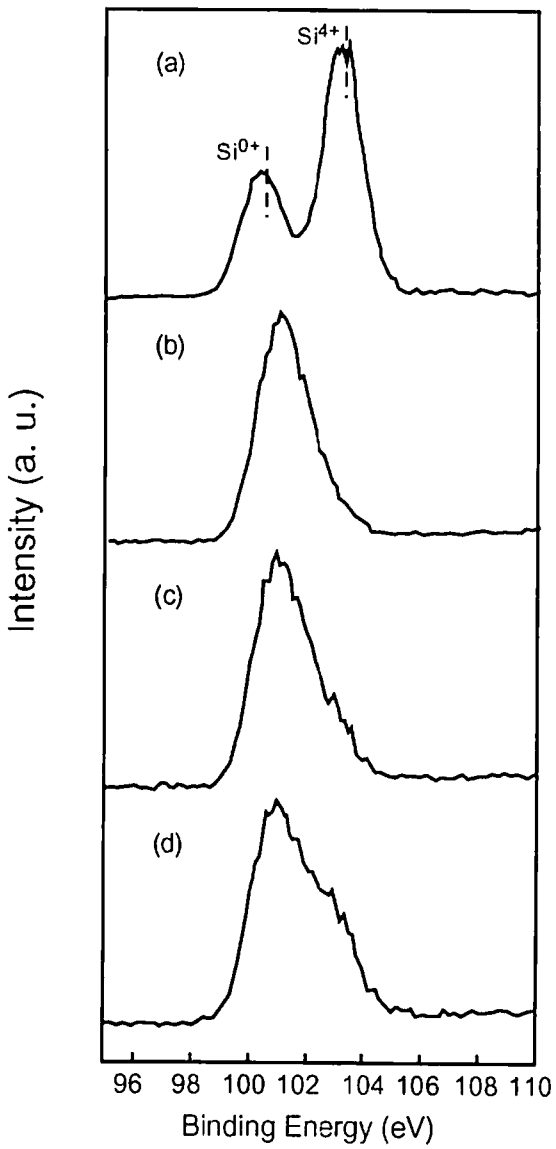

Fig. 6. 5. XPS spectra of Si2p of the SiC surface: (a) illuminated with the TiO_2; (b) with the TiO_2 in dark; (c)illuminated ($\lambda > 440$ nm) with the TiO_2; and (d) illuminated without the TiO_2.

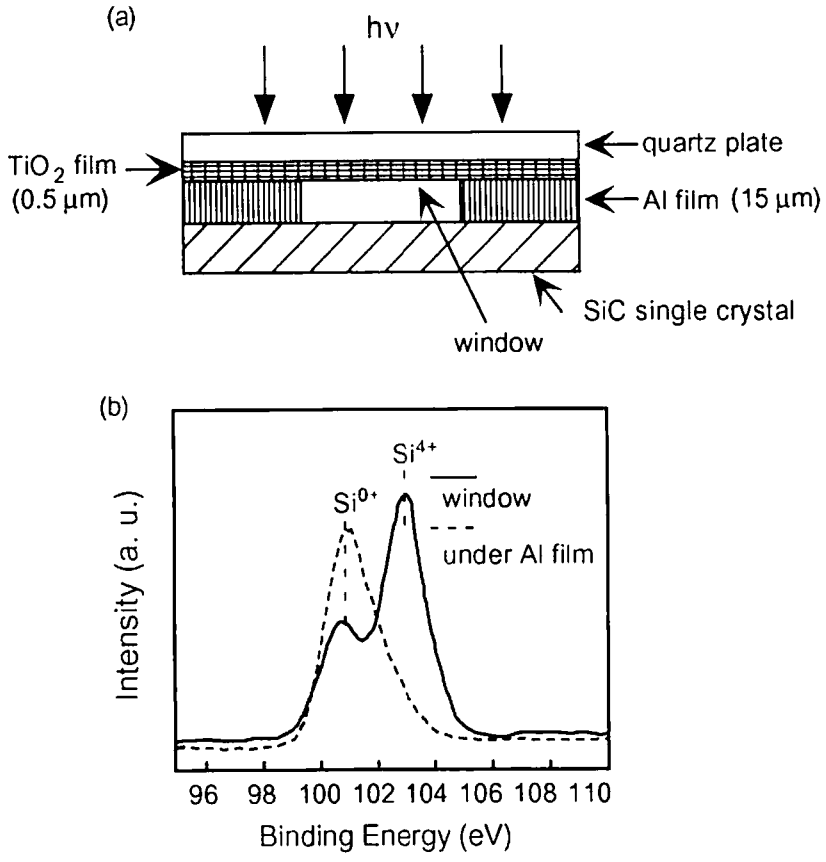

Fig. 6. 6. Model for the non-contact photocatalytic oxidation of the SiC single crystal (a) and XPS spectrum of Si2p of the SiC illuminated with non-contacted TiO_2 (b).

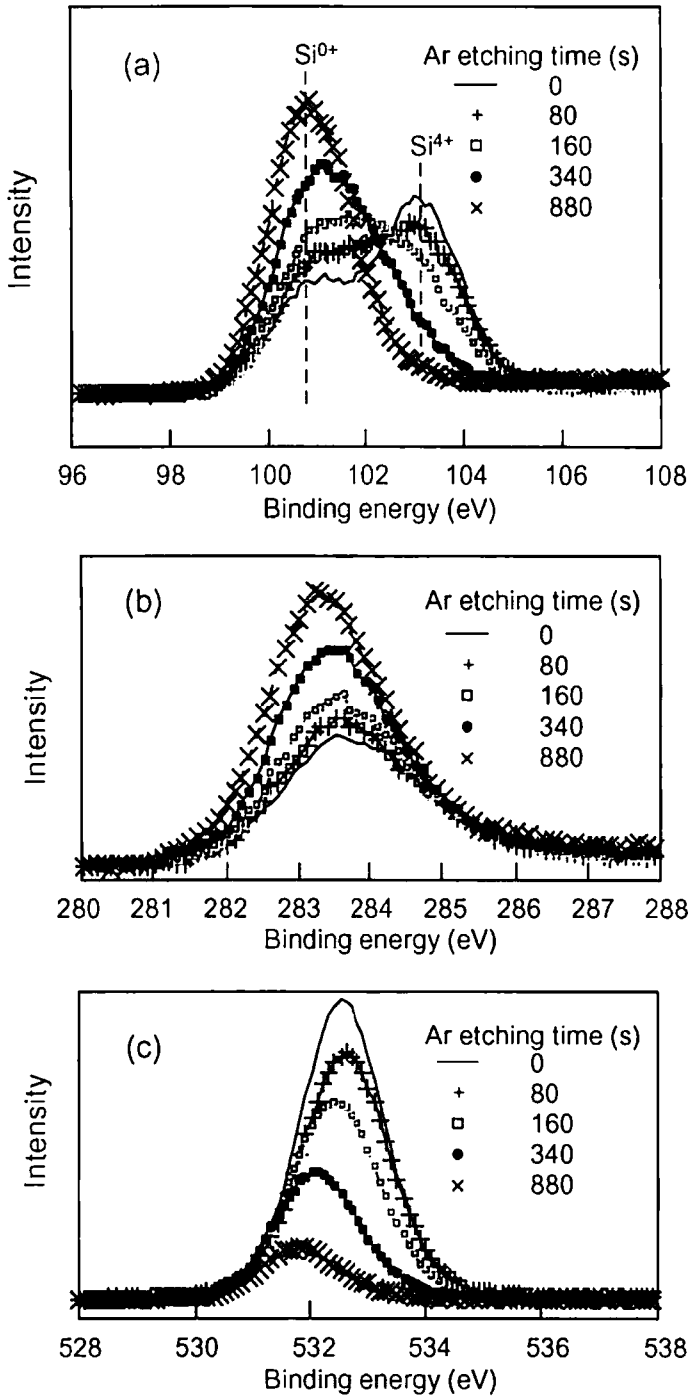

Fig. 6. 7. XPS spectra of the SiC surface after the TiO_2 photocatalysis test under illumination for 1 h: (a) Si2p, (b) C1s, and (c) O1s. Ar etching was done at the etching rate of 0.5 A/sec.

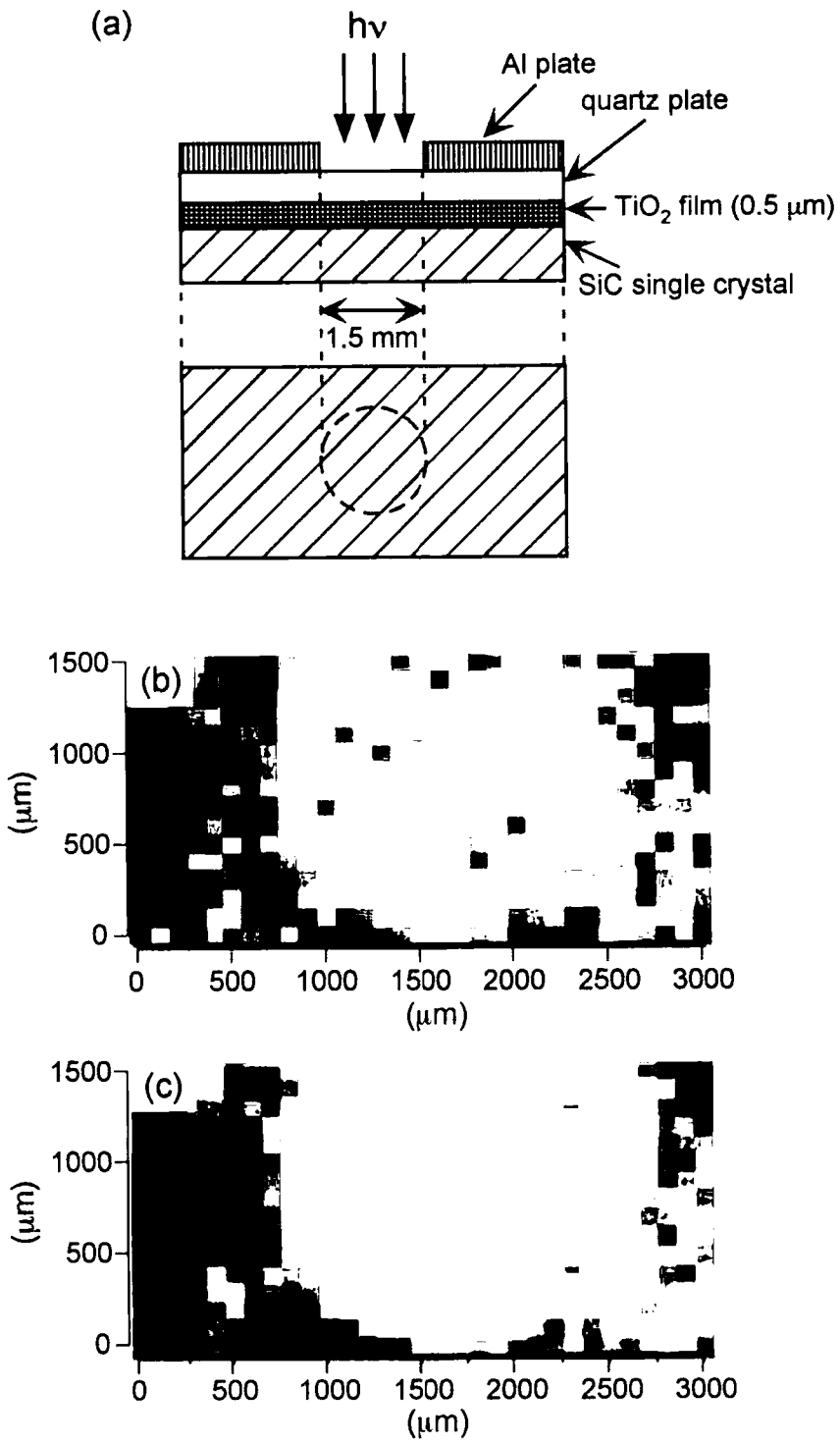

Fig. 6. 8. Model for the photo-patterning test of the SiC single crystal (a) and spectrum intensity mapping of $Si^{4+}2p$ (b) and O1s (c) on the SiC.

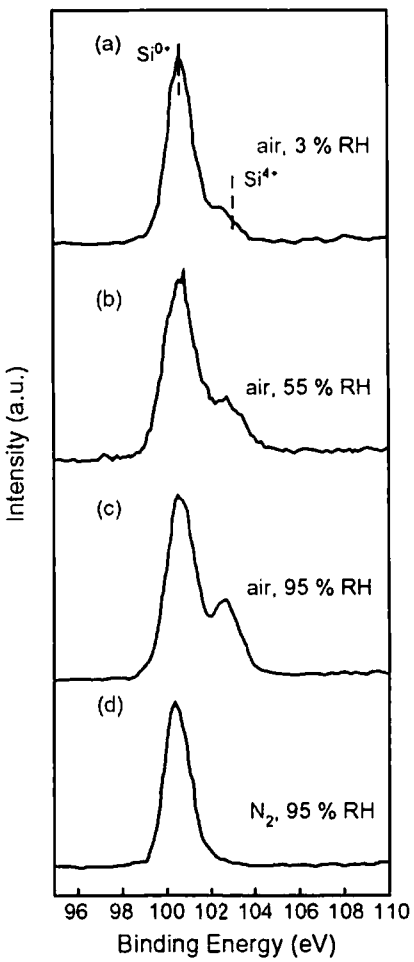

Fig. 6. 9. XPS spectra of Si2p of the SiC surface after the surface treatment under illumination by the remote system (Fig. 6. 2) using various gases: (a) air with 3 % RH; (b) air with 55 % RH; (c) air with 95 % RH; (d) N_2 with 95 % RH.

Chapter 7

General Conclusion

In this thesis, the preparation of TiO_2 photoatalyst film fixed on alumite and the surface treatment of inorganic solid materials using TiO_2 photocatalytic reaction have been studied.

Each chapter is summarized as follows.

Chapter 1 Introduction

In this chapter, the general background of the present thesis was reviewed and aims of the studies were described.

Part I: Preparation of TiO_2 Photocatalyst on Alumite Substrate.

In this part, the preparation of TiO_2 photocatalyst film fixed alumite ($Al/Al_2O_3/TiO_2$) was described, and the characterization and the photocatalytic activity of that were demonstrated. Moreover, the mechanisms of TiO_2 deposition were discussed.

Chapter 2 A New Electrochemical Method to Prepare Mesoporous Titanium(IV) Oxide Photocatalyst Fixed on Alumite Substrate

TiO_2 film was deposited onto alumite using an electrochemical technique, where the initial electrodeposition was carried out by ac electrolysis in $(NH_4)_2[TiO(C_2O_4)_2]$ solution, followed by pulse electrolysis in $TiCl_3$ aqueous solution. The sizes of the TiO_2 particles in the prepared film were about 5 nm, and they consisted of mixtures of the anatase, rutile and amorphous phases. This film had extremely high

catalytic activity for the decomposition of acetaldehyde even under weak fluorescent lamp illumination. The preparation cost is very low compared with other methods. Therefore, the prepared alumite fixed with TiO_2 photocatalys by present method is very useful for the practical photodecomposition of chemical contaminant in the atmosphere.

Chapter 3 Electrodeposition of TiO_2 photocatalyst into nano-pores of hard alumite

TiO_2 was electrodeposite into the pores of hard alumite by alternative electrolysis in $(NH_4)_2[TiO(C_2O_4)_2]$ solution, where the alumite was prepared by anodic oxidation of aluminum in sulfuric acid at 2-4 °C (hard alumite). When the electrolysis was carried out in an $(NH_4)_2[TiO(C_2O_4)_2]$ solution under ac bias for the hard alumite, a cathodic current due to the reduction of H^+ and/or H_2O was observed at about –10 V in measurement of the Lissajous figure, leading to the deposition of TiO_2. Consequently, the TiO_2 was deposited during an increase in pH due to the electrochemical reduction reaction of H^+ and/or H_2O in pores of the alumite. The deposited TiO_2 was highly dispersed in the pores of the alumite, leading to strong adhesion between the deposited TiO_2 and the alumite. The prepared TiO_2 in the pores of the alumite ($Al/Al_2O_3/TiO_2$) showed high photoatalytic activity for the decomposition of acetaldehyde compared to TiO_2 deposited direlcty of an aluminum surface (Al/TiO_2).

Chapter 4 Preparation of Titanium(IV) Oxide Film on Hard Alumite Substrate

TiO_2 was deposited onto hard alumite ($Al/Al_2O_3/TiO_2$) by alternating current electrolysis and precipitation in $(NH_4)_2[TiO(C_2O_4)_2]$ solution at various temperatures, where the hard alumite was prepared by the anodic oxidation of aluminum in sulfuric acid (Al/Al_2O_3). The TiO_2 electrodeposition mainly occurred at temperatures lower than about 50 °C, while the TiO_2 deposition due to $TiO(C_2O_4)_2^{2-}$ adsorption onto alumite predominantly occurred at temperatures higher than about 50 °C. The amount of

deposited TiO_2 increased with the increase in the deposition temperature, leading to high photoatalytic activity for the decomposition of acetaldehyde even under weak fluorescent lamp illumination. The $Al/Al_2O_3/TiO_2$ prepared at 50 °C was optimal for practical use, because of a relatively high activity and the sufficient adhesion strength between the TiO_2 and Al/Al_2O_3 substrate due to the presence of the deposited TiO_2 in the pores of the alumite film.

Chapter 5 Electrodeposition of TiO_2 Photocatalyst into Porous Alumite Prepared in Phosphoric Acid

TiO_2 was electrodeposited into the pores of the alumite by alternative electrolysis in $(NH_4)_2[TiO(C_2O_4)_2]$ solution ($Al/Al_2O_3/TiO_2$), where the alumite was prepared by anodic oxidation of aluminum in phosphoric acid solution. The applied ac voltage to deposit TiO_2 was high in the alumite prepared in phosphoric acid, compared with that in the case of sulfuric acid solution, because the alumite formed in phosphoric acid solution has a barrier layer thicker than that of the alumite formed in sulfuric acid solution. The particle size of the deposited TiO_2 was less than 2 nm. The $Al/Al_2O_3/TiO_2$ prepared in this study showed high photocatalytic activity for the decomposition of acetaldehyde.

Part II: Surface Treatment of Inorganic Materials Using TiO_2 Photoatalytic Reaction.

Chapter 6 Surface Treatment of Diamond and Silicon Carbide Using Titanium(IV) Oxide Photocatalyst

Silicon carbide and diamond were decomposed to produce $CO_2(g)$ by the photocatalytic reaction of TiO_2 at room temperature. According to the XPS spectra of Si2p on the SiC surface, SiO_2 was simultaneously formed on the surface by the TiO_2

photocatalysis. The thickness of the SiO_2 formed on the SiC surface during the photocatalysis for 1h was estimated to be about 40 Å based on the depth profile of the XPS spectra using Ar etching. The SiC surface was oxidized by the TiO_2 photocatalysis even with no contact of the TiO_2, indicating that the photocatalytic oxidation of the SiC occurred due to active oxygen species photogenerated on the TiO_2 surface, and not direct oxidation by the photogenerated hole in the valence band of TiO_2. The photocatalytic decomposition of the diamond powder slowly proceeded, where about 1 % of the C atom of the diamond surface was decomposed to $CO_2(g)$ in 2 h.

The important points proposed in the present thesis are summarized as follows:

Part I. New electrochemical preparation and fixation of TiO_2 onto the Al/Al_2O_3 substrate ($Al/Al_2O_3/TiO_2$) was developed. These had an excellent photocatalytic activity. Moreover, the present easily method to prepare $Al/Al_2O_3/TiO_2$ is low in cost. Therefore, the $Al/Al_2O_3/TiO_2$ will be usually used as a cheap building material.

Part II. New application of TiO_2 photocatalyst to the surface treatment of the inorganic solid material was developed. In this application, micro-level and photo-patterning will also be possible. Moreover, the TiO_2 photocatalytic reaction will be very useful for the surface treatment of inorganic materials without defects and damage to the substrate, because the reaction is carried out under mild conditions.